Loss of endothelial miR-126 drives age-related decline in hematopoiesis

Dandan Zhao,[1*] Le Xuan Truong Nguyen,[1*] Xubo Gong,[1,2*] Fang Chen,[1] Xiaoli Zhao,[1] Min-Hsuan Chen,[3] Guido Marcucci[1] and Bin Zhang[1]

[1]Department of Hematological Malignancies Translational Science, Gehr Family Center for Leukemia Research, City of Hope National Medical Center and Beckman Research Institute, Duarte, CA, USA; [2]Department of Clinical Laboratory, The Second Affiliated Hospital, Zhejiang University School of Medicine, Hangzhou, Zhejiang, P.R. China and [3]Integrative Genomics Core, Department of Computational and Quantitative Medicine, City of Hope Beckman Research Institute, Duarte, CA, USA

**DZ, LXTN and XG contributed equally as first authors.*

Correspondence: B. Zhang
bzhang@coh.org

G. Marcucci
gmarcucci@coh.org

Received: July 17, 2025.
Accepted: November 25, 2025.
Early view: December 4, 2025.

https://doi.org/10.3324/haematol.2025.288736

Loss of endothelial miR-126 drives age-related decline in hematopoiesis

Dandan Zhao, Le Xuan Truong Nguyen, Xubo Gong, Fang Chen, Xiaoli Zhao, Min-Hsuan Chen, Guido Marcucci, Bin Zhang

Supplemental Methods

Mouse strains

Unless otherwise indicated, 2-3 months old and 18-24 months old C57Bl/6J (B6, CD45.2) mice were used as young and aged mice respectively. *Tie2-CreER/TdTomato/Tg(Ly6a-GFP)* double fluorescent endothelial cell(EC)/Sca-1 reporter mice[1], generated by crossing *Tie2-CreER/TdTomato* mice (CD45.2 B6), in which BM ECs bearing the Tie2-promoter driven TdTomato color upon tamoxifen administration (EC-tdTomato^{+}, EC reporter mice)[2,3], with *Tg(Ly6a-EGFP)* (Sca-1-GFP^{+}, Sca-1 reporter mice, from The Jackson Laboratory, 012643), were used to allow us to visualize Sca-1^{high} EC (tdTomato^{+}GFP^{high}) and Sca-1^{low} EC (tdTomato^{+}GFP^{low}) lined vessels based on the combined expression of these two endogenous reporters. *Mir126$^{flox(f)f}$Tie2-cre*+ [i.e., EC-miR-126 knock-out (KO)] and *Spred1$^{f/f}$Tie2-cre*+ (EC-Spred1 KO, representing a functional EC-miR-126 overexpressing model) mice[1,4] were used to obtain miR-126 KO or overexpression in ECs. To obtain conditional EC miR-126 KO reporter mice, we also bred *Tie2-CreER/TdTomato* reporter mice with *Mir126$^{f/f}$* mice and obtained inducible EC miR-126 KO reporter mice (i.e., *Mir126$^{f/f}$/Tie2-CreER/TdTomato*, miR-126 KO in ECs upon tamoxifen administration; tamoxifen: from Sigma-Aldrich, CAS # 10540-29-1; 75mg/kg in corn oil solution, ip injection, once every 24 hours for a total of 4 consecutive days). Mouse care and experimental procedures were performed in accordance with federal guidelines and protocols and were

approved by the Institutional Animal Care and Use Committee at the City of Hope (under the approved protocol IACUC 15005).

Immunofluorescent staining and 3D confocal imaging of long bones

Long bones (tibias) from the mice were processed, sectioned, and imaged as described previously[1,4,5]. Briefly, the bone was dissected from mice and surrounding muscle was removed without causing any mechanical damage to bones. The dissected bone was immediately fixed with 4% paraformaldehyde (PFA) for 4 hours. Then, the bone was washed three times with PBS at 4^0C and processed for decalcification. It was incubated in decalcification solution (0.5M EDTA, pH 7.4-7.6) for 24 to 48 hrs, washed three times with PBS and continuously incubated with ice-cold cryoprotectant (CPT) solution at 4^0C for 24 hrs. After incubating with embedding media for 45 minutes (min) at 60^0C in a water bath, the bone was embedded in a tissue mold, which was dried at room temperature (RT) for 30 min and stored at -80^0C at least over night until sectioning. Tissue sections were cut at -23^0C using a microtome with a thickness of 40 µm and transferred to a microscope slide for staining. The sections were rehydrated with PBS at RT for 5 min, incubated with permeabilization solution for 20 min, and blocked with freshly made blocking solution containing BSA for 30 min. The slides were incubated with fluorescent conjugated Abs (CD31-FITC/Sca-1-PE or CD31-PE/Endomucin-FITC; 1:250 dilution) overnight at 4^0C. Then, the slides were washed with PBS and nuclear staining was performed with 4′,6-diamidino-2-phenylindole (DAPI, BD) mounting solution. Imaging was performed using a confocal microscope (Zeiss, LSM880) and analyzed using the Zen program (Zeiss). We also performed high-resolution

3D confocal imaging using long bones from EC/Sca-1 reporter mice [i.e., tamoxifen-treated Tie2-CreER/TdTomato/Tg(Ly6a-GFP)], which allow us to visualize Sca-1^{high} EC (i.e., tdTomato^{+}GFP^{high}) and Sca-1^{low} EC (i.e., tdTomato^{+}GFP^{low}) lined vessels. To distinguish vessel subtypes, CD31^{+}Emcn^{high} EC-lined vessels located in metaphysis of the long bone with a narrow, elongated morphology and continuous endothelial lining were defined as type H vessels; CD31^{+}Sca-1^{high} EC-lined vessels located in metaphysis and diaphysis of long bones with a narrow, elongated morphology and continuous endothelial lining were defined as arterioles; and CD31^{+}Sca-1^{low} EC-lined and highly branched vessels located in diaphysis with a thin wall were defined as sinusoids, as indicated in the schematic diagram (see Figure S3A) and reported previously by us[1,4]. To quantify Sca-1^{high} EC-lined arterioles in the images, we used a threshold of 80 as a cutoff for the Sca-1-PE or GFP channel. Briefly, connected objects of Sca-1-PE or -GFP signals were identified and those with fewer than 15 pixels were removed to reduce noise using MATLAB's bwareafilt function[1,4]. The image was then morphologically closed with a 1.0-pixel filter using MATLAB's imclose function to close any holes. The perimeter:area ratio was calculated for each object; objects with a ratio of less than 0.7 were removed using MATLAB's bwconncomp and bwperim functions. The goal was to identify blood vessels as they are thinner than other objects in the image. Finally, the fractions of pixels (i.e., arbitrary unit) that registered as positive for blood vessels within three representative hand-drawn regions of interest were reported as the quantification of arterioles, as reported by us previously[1].

Intravital vascular permeability imaging

Intravital confocal microscopy was used to image the calvarium BM vasculature to study the vascular permeability, as previously described[1,6]. Briefly, mice were anesthetized using intraperitoneal injection of saline solution containing 120 mg/kg ketamine, 10 mg/kg xylazine, and 3 mg/kg acepromazine. After confirming proper anesthesia by checking for foot reflex, we applied eye ointment to keep the eyes moist during surgery. Prior to imaging, mice were injected intravenously with fluorescent dextran (i.e., FITC-150kDa dextran). We shaved the head, revealed the calvaria by a skin incision and held it in a stereotaxic skull holder. Then image acquisition was performed using a Zeiss LSM880 confocal microscope (AxioObserver platform) equipped with a Plan-Apochromat 10×/0.45 M27 objective. Image acquisition was performed in fluorescence contrast mode with the pinhole set at 0.72 Airy units to optimize optical sectioning. Scans were acquired in frame mode with unidirectional scan direction and a scan zoom of 1.0. The detection system was configured with standard photomultiplier tube (PMT) detectors, and the digital gain was maintained at 1.0 to minimize acquisition-related variability. For volumetric imaging, z-stacks were collected across a depth of 100 μm with 12 optical slices per stack, providing a z-interval of approximately 8–9 μm. To capture a larger field of view, images were tiled (4 tiles per acquisition) and stitched during processing.

Raw images were imported into ZEN Lite (Carl Zeiss, version 3.3) for post-acquisition processing and quantitative analysis. Parameters such as fluorescence intensity distribution, vessel segmentation, and dye extravasation were measured using the built-in tools, and representative images were generated without further manipulation beyond linear adjustments to brightness and

contrast. Vascular permeability was quantified by the dextran leakage (i.e., dextran diffusion) from the vessels using Zen Lite 3.3 software (Zeiss). For each group of mice, 10 random regions of interest (ROIs) were selected outside the vessel wall using a fixed-size square box. The green fluorescence intensity within each ROI, after subtracting the background fluorescence, was used to assess extravascular dextran leakage.

Measurement of cytokine and chemokine levels in mouse blood and marrow by Luminex Assay

Blood and marrow plasmas were collected from young (2-3 months old; n=8 for blood plasma and n=10 for marrow plasma) and aged (15-20 months old; n=8 for blood plasma and n=14 for marrow plasma) mice. 0.5ml peripheral blood per mouse was collected and plasma was obtained. BM cells were flushed from the femurs of each mouse using 200 μL IMDM. BM cell suspension was centrifuged, and supernatants were collected. Luminex immunoassay for a panel of 33 murine cytokines and chemokines [R&D mouse 33 Plex: Angiopoietin-2, CRG-2 (CXCL10), EGF, Eotaxin, FGF21, FGF2, G-CSF, GM-CSF, IFN-γ, IL-1α, IL-1β, IL-3, IL-4, IL-10, IL-12 (p70), IL-13, IL-16, KC, LIX (CXCL5), M-CSF, MCP-1, MCP-5 (CCL7), MIP-1α (CCL3), MIP-1β, MIP-2, MIP-3α, RANTES (CCL5), SDF-1α (CXCL12), TNF-α, TNFSF12, TNFSF13B, TNFSF6, VEGF] were performed with blood plasma and BM supernatants and concentrations calculated using standard curves. The volume of the BM cavities of two femurs is approximately 20 μL, and the measured concentration of cytokines was adjusted based on this dilution factor (200/20= 10x) to obtain the concentration of cytokines per unit volume BM.

Isolation and culture of endothelial cells from long bones

ECs were isolated from long bones (tibias and femurs) of the mice as previously described[1]. Briefly, after removing the muscle and connective tissue, the bones were flushed using a 23-gauge needle and 3 ml of cold Iscove's Modified Dulbecco's Medium (IMDM, ThermoFisher) and collected as central marrow. The marrow-depleted bones were crushed gently with a mortar and pestle in cold IMDM and the bone fragments were incubated at 37 °C with 3ml of 3mg/ml collagenase I (Sigma) and gently agitated for 45 min. The digested bones were then filtered through a 40 μm strainer (BD Bioscience) and collected as endosteal marrow. Central marrow and endosteal marrow were combined and then stained and analyzed by flow cytometry. $CD45^-$ $Ter119^-CD31^+$ ECs and $Sca\text{-}1^{high}$ and $Sca\text{-}1^{low}$ subfractions were also sorted by flow cytometry for *in vitro* cultures. Mouse BM ECs were cultured in complete EGM-2 medium (CC-3162, Lonza), at 37°C with 5% CO_2 and 21% O_2 and high humidity.

Flow cytometry analyses

Mouse cells were obtained from PB or BM (from both tibias and femurs). Before staining for hematopoietic stem cells (HSCs), $c\text{-}Kit^+$ cells were selected using anti-mouse CD117 microbeads or $Lineage^-$ (Lin^-) cells were selected using mouse Lineage cell depletion kit (both from Miltenyi Biotec, San Diego, CA). The following mouse antibodies were used: mouse biotinylated lineage markers (Ter-119, CD3, NK1.1, IgM, CD4, CD8a, CD19, Gr-1, CD11b, B220), CD45-PE or FITC or APC-eflu780, Ter119-APC-eflu780, CD31-PE-cy7 or APC, Flt3-biotin or PE, CD117 (c-Kit, ACK2 clone or 2B8 clone)-APC-eFlu780, Sca-1-PE or PE-Cy7, CD150-PE, CD48-APC or pacific

blue, and streptavidin-PE or FITC or PerCP-Cy5.5 (all from eBioscience, San Diego, CA; see Table S1). HSCs were identified as $Lin^{-}Sca\text{-}1^{+}c\text{-}Kit^{+}(LSK)Fit3^{-}CD150^{+}CD48^{-}$. ECs were identified as $CD45^{-}Ter119^{-}CD31^{+}$. Sca-$1^{high}$ and Sca-1^{low} EC subfractions from *in vitro* studies and from *in vivo* studies were analyzed. To determine negative and positive populations in flow cytometry plots, we have used a combination of controls, including unstained samples to set the background fluorescence, isotype controls to determine background levels of non-specific binding, Fluorescence Minus One (FMO) controls to account for spectral spillover in multicolor panels, to define a gate on a plot that separates the brightly stained "positive" cells from the dimmer "negative" cells. All analyses were performed on a Fortessa x20 flow cytometer (BD Biosciences) and sorting was performed on Aria Fusion instrument (BD Biosciences) and data were analyzed by BD FACSDiva or FlowJo software.

Luciferase reporter assay

Spred1 3' UTR or 3' UTR with mutations engineered in the region complementary to the miR-126 seed region (GGTACGA to TTGGAAG; 3' UTR-m), was inserted into the psiCHECK-2 vector (Promega). Mouse endothelial cells (C166, from ATCC) were co-transfected with psiCHECK-2 containing the Spred1 3' UTR or 3' UTR-m plasmids. After transfection (48 hrs), the activities of firefly and Renilla luciferases were measured sequentially from a single sample using the Dual-Luciferase® Reporter Assay System (Promega, E1910) according to the manufacturer's protocol. Briefly, cultured cells were rinsed with 1× PBS and lysed by 1× Passive Lysis Buffer (PLB) solution (Promega, E1941). Homogeneous lysates were prepared by manually scraping the cells from

culture wells in the presence of 1× PLB and then transferred into a tube. The firefly luciferase reporter is measured first by adding Luciferase Assay Reagent II (LAR II) to generate a stabilized luminescent signal. After quantifying the firefly luminescence, this reaction is quenched, and the Renilla luciferase reaction is simultaneously initiated by adding Stop & Glo® Reagent to the same tube and then measured Renilla luminescence. Measurements were read using a white, flat bottom 96-well plate (Costar, 3912) on a GloMax® 20/20 Luminometer. The normalized luciferase ratio is obtained for each well by calculating “firefly reporter activity/Renilla reporter activity”.

Transplant experiment

To evaluate the impact of intrinsic versus (vs) extrinsic factors on self-renewal and repopulating capacities of aging HSCs, BM HSCs (Fit3$^-$CD150$^+$CD48$^-$ LSK) were sorted from 2-3 or 18-24 months old CD45.2 B6 mice and transplanted into 2-3 or 18-24 months old CD45.1 B6 mice (200 cells/mouse or 2,000 cells/mouse). To evaluate the impact of EC miR-126 depletion on HSC self-renewal capacity, BM HSCs (200 cells/mouse) were also sorted from 2-3 months old *Mir126$^{f/f}$/Tie2-cre*+ or *Mir126$^{f/f}$/Tie2-cre*- mice or from 18-24 months old *Spred1$^{f/f}$/Tie2-cre*+ or *Spred1$^{f/f}$/Tie2-cre*- mice (all CD45.2 B6) and transplanted into congenic recipient mice (CD45.1 B6, from Charles River, B6-Ly5.1, Kingston, US). Unless otherwise indicated, CD45.1 B6 recipient mice used in this study were 2-3 months old male and female mice and were irradiated at 6 Gy (X-RAD 320 irradiator) within 24 hours before transplantation, to achieve complete myeloablation enabling engraftment. Congenic CD45.1 BM cells (2x10^5 per mouse) were co-transplanted with LT-HSC to help the recipient mice survive myeloablation following irradiation. The number of mice

for each study group was chosen based on the expected endpoint variation (i.e., engraftment rate) and on the availability of mice from different strains. All animals studied were compared within litters and/or age- and sex-matched. Mice of the same gender and age were randomly divided into groups.

RNA sequencing

Total RNA was extracted from BM HSCs ($Fit3^{-}CD150^{+}CD48^{-}$ LSK) sorted from young (n=30) and aged (n=3) mice using the miRNeasy micro Kit (Qiagen, Valencia, CA). Sequencing libraries were prepared from approximately 1.5 ng of total RNA using the NEBNext® Single Cell/Low Input RNA Library Prep Kit (New England Biolabs, Cat. E6420S), following the manufacturer's protocol. Final libraries were quantified using a Qubit fluorometer and assessed for fragment size distribution with an Agilent Bioanalyzer. Sequencing was performed on an Illumina NovaSeq 6000 platform using the S4 Reagent Kit v1.5 in paired-end mode (2 × 101 cycles). Base calling was carried out using Real-Time Analysis (RTA) software version 3.4.4.

To minimize background noise and improve the reliability of downstream analyses, genes with very low expression were excluded. Specifically, only genes with an RPKM value of 1 or higher in two or more samples from either the young or aged HSC group were retained. A quality control heatmap based on these filtered genes revealed consistent expression profiles across both age groups. Unsupervised clustering showed that samples grouped according to biological age rather than technical factors such as batch or sample origin. This indicates that the variation in the data is primarily driven by biological differences, with minimal influence from technical artifacts. The

absence of clustering by batch or processing conditions further confirms that the study design and normalization procedures successfully reduced batch-related variability. Therefore, no additional batch effect correction was required. RNA-Seq reads were trimmed to remove sequencing adapters using Trimmomatic[7] and polyA tails using FASTP[8]. The processed reads were mapped back to the mouse genome (mm10) using STAR software (v. 2.6.0.a)[9]. The HTSeq software (v.0.11.1)[10] was applied to generate the count matrix, with default parameters. Differential expression gene (DEG) analysis was conducted by adjusting read counts to normalized expression values using TMM normalization method in edgeR[11,12]. Briefly, general linear models were applied to identify DEGs between the aged and the young HSCs using TMM normalization expression level as a depending variable, and age difference as an independent variable. Genes with an FDR-adjusted p-value less than 0.05 and with a fold change (FC) greater than 2 or less than 0.5 were considered as significant up- and down-regulated genes, respectively. Gene set enrichment analysis (GSEA) was conducted using the HALLMARK and KEGG datasets, the well-curated gene set collections from the Molecular Signatures Database (MSigDB). The analyses utilized the HALLMARK gene sets (h.all.v2022.1.Hs.symbols.gmt) and the KEGG canonical pathways (c2.cp.kegg.v2022.1.Hs.symbols.gmt) to capture key biological processes and pathways. Consistent with recommendations in the official GSEA user guide, a false discovery rate (FDR) threshold of 25% (FDR < 0.25) was applied to determine significantly enriched gene sets, a standard criterion for exploratory analyses. Pathway analysis was conducted using GSEA algorithm implemented in clusterProfiler (v.4.14.3) package in R[13-16], where a ranked list of whole genes according to their log2 fold change and p-values are provided.

Chromatin immunoprecipitation (ChIP)

GATA2 binding to DNA sequence upstream of EGFL7/miR-126 was analyzed by ChIP assay using the MAGnify ChIP system (ThermoFisher) according to the manufacturer's protocol. Briefly, endothelial cells were crosslinked and sheared to fragments by sonification to ~500-2000 bp. Magnetic beads were incubated with 5 µg control IgG or anti-GATA2 antibody-ChIP Grade (Abcam, ab22849) for 1 hour at room temperature before lysate was incubated with bead-antibody complex for 1 hour at 4°C. After washing and reverse crosslinking, DNA was purified using DNA purification spin columns, followed by quantitative real-time PCR. Fold enrichment was calculated with equation: 2^(ΔCt) method (ΔCt=Ct of IP sample – Ct of IgG sample).

RNA isolation and Q-RT-PCR

Total RNA, including miRNA, was extracted using the miRNeasy Mini or micro Kit (Qiagen, Valencia, CA) following the manufacturer's protocol. For mRNA and pri- and pre-miR-126 expression, first-strand cDNA was synthesized using the SuperScript III First-Strand Kit and then quantitative real-time PCR (Q-RT-PCR) was performed using Taqman gene expression assays (ThermoFisher, pri-miR-126: Mm03306244_pri; pre-miR-126: Mm04335191_s1; see Table S2). For mature miR-126 expression, reverse transcription were performed using SuperScript™ IV Reverse Transcriptase (Thermo Fisher Scientific, 18090010) and Applied Biosystems® TaqMan® MicroRNA Reverse Transcription Kit (Thermo Fisher Scientific, 4366596) and the gene specific primers provided by TaqMan® MicroRNA Assay (ThermoFisher, assay ID: 2228; see Table S2),

followed by Q-PCR analysis using Taqman assays, according to the manufacturer's protocol. *β2m* were used as internal controls for mRNA and pri/pre miR-126 and snoRNA234 as internal controls for mature miR-126. Results are presented as log2-transformed ratio according to the $2^{-\Delta Ct}$ method (ΔCt=Ct of target –Ct of control).

Oligonucleotide design and synthesis

MiR-126 mimic oligonucleotide was designed and synthesized as previously described[1,17]. Briefly, miR-126 mimic or scramble RNA (scrRNA, control) was linked with the partially phosphorothioated oligodeoxyribonucleotide (ODN) using 5 units of C3 carbon chain linker, (CH2)3 (indicated by x), and generated the miR-126 mimic passenger. The guide and passenger oligonucleotides were then mixed and heated to 80°C for 1 min, followed by incubating at 37°C for 1 h, to generate miR-126 mimics. The sequences were as follows: **miR-126-3p-mimic (guide)**: 5'- rUrCrGrUrArCrCrGrUrGrArGrUrArArUrArArUrGrCrG-3'; **CpG-miR-126-3p-mimic (passenger)**: 5'-G*G*TGCATCGATGCAGG*G*G*G*Gxxxxx rCrArUrUrArUrUrArCrUrCrArCrGrGrUrArCrGrAmArA-3'; **Scramble RNA (SCR, guide)**: 5'-rGrGrCrGrUrGrUrArUrUrArArGrGrCrUrArArArUrCrU-3'; **CpG-SCR (passenger)**: 5'-G*G*T GCATCGATGCAGG*G*G*G*G xxxxx rArUrUrUrArGrCrCrUrUrArArUrArCrArCrGrCrCmArA-3', where the asterisk (*) indicates phosphorothioation. One nonbridging atom of oxygen on phosphate was replaced with sulfur. 'r' indicates ribo. 'm' indicates the 2′-O-methyl analog of the nucleotide.

References

1. Zhang B, Nguyen LXT, Zhao D, et al. Treatment-induced arteriolar revascularization and miR-126 enhancement in bone marrow niche protect leukemic stem cells in AML. J Hematol Oncol. 2021;14(1):122.
2. Hochstetler CL, Feng Y, Sacma M, et al. KRas(G12D) expression in the bone marrow vascular niche affects hematopoiesis with inflammatory signals. Exp Hematol. 2019;79:3-15 e14.
3. Feng Y, Liu M, Guo F, et al. Novel Method to Study Mouse Bone Marrow Endothelial Cells in Vivo and in Vitro. Blood. 2012;120(21):617-617.
4. Qiao J, Zhao D, Nguyen LXT, et al. Targeting miR-126 in Ph+ acute lymphoblastic leukemia. Leukemia. 2023;37(7):1540-1544.
5. Kusumbe AP, Ramasamy SK, Starsichova A, Adams RH. Sample preparation for high-resolution 3D confocal imaging of mouse skeletal tissue. Nat Protoc. 2015;10(12):1904-1914.
6. Passaro D, Di Tullio A, Abarrategi A, et al. Increased Vascular Permeability in the Bone Marrow Microenvironment Contributes to Disease Progression and Drug Response in Acute Myeloid Leukemia. Cancer Cell. 2017;32(3):324-341 e326.
7. Bolger AM, Lohse M, Usadel B. Trimmomatic: a flexible trimmer for Illumina sequence data. Bioinformatics. 2014;30(15):2114-2120.
8. Chen S, Zhou Y, Chen Y, Gu J. fastp: an ultra-fast all-in-one FASTQ preprocessor. Bioinformatics. 2018;34(17):i884-i890.
9. Dobin A, Davis CA, Schlesinger F, et al. STAR: ultrafast universal RNA-seq aligner. Bioinformatics. 2013;29(1):15-21.
10. Anders S, Huber W. Differential expression analysis for sequence count data. Genome Biol. 2010;11(10):R106.
11. McCarthy DJ, Chen Y, Smyth GK. Differential expression analysis of multifactor RNA-Seq experiments with respect to biological variation. Nucleic Acids Res. 2012;40(10):4288-4297.
12. Robinson MD, McCarthy DJ, Smyth GK. edgeR: a Bioconductor package for differential expression analysis of digital gene expression data. Bioinformatics. 2010;26(1):139-140.
13. Wu T, Hu E, Xu S, et al. clusterProfiler 4.0: A universal enrichment tool for interpreting omics data. Innovation (Camb). 2021;2(3):100141.
14. Xu S, Hu E, Cai Y, et al. Using clusterProfiler to characterize multiomics data. Nat Protoc. 2024;19(11):3292-3320.
15. Yu G. Thirteen years of clusterProfiler. Innovation (Camb). 2024;5(6):100722.
16. Yu GC, Wang LG, Han YY, He QY. clusterProfiler: an R Package for Comparing Biological Themes Among Gene Clusters. Omics-a Journal of Integrative Biology. 2012;16(5):284-287.
17. Zhang B, Nguyen LXT, Li L, et al. Bone marrow niche trafficking of miR-126 controls the self-renewal of leukemia stem cells in chronic myelogenous leukemia. Nat Med. 2018;24(4):450-462.

Statistical analysis

All statistical analyses were performed using Prism version 10.0 software (GraphPad Software). Sample sizes chosen are indicated in the individual figure legends. All the in vitro experiments were performed 2-3 times using biologically independent samples; the in vivo experiments were performed using 6–16 mice in each group. Results shown represent mean ± SEM or SD. Comparisons between groups were performed by a two-tailed, unpaired Student's t-test.

Supplementary Tables and Figures

Table S1. Antibodies used in this study

Anti-mouse antibodies used for flow cytometry analysis				
Name	**color**	**manufacturer**	**clone**	**cat**
CD3e	biotinylated	eBioscience	145-2c11	13-0031-85
CD4	biotinylated	eBioscience	GK1.5	13-0041-85
CD8a	biotinylated	eBioscience	53-6.7	13-0081-85
B220	biotinylated	eBioscience	RA3-6B2	13-0452-85
CD19	biotinylated	eBioscience	eBio1D3 (1D3)	13-0193-85
IgM	biotinylated	eBioscience	II/41	13-5790-85
Gr-1	biotinylated	eBioscience	RB6-8C5	13-5931-85
CD11b	biotinylated	eBioscience	M1/70	13-0112-85
NK1.1	biotinylated	eBioscience	PK136	13-5941-85
Ter119	biotinylated	eBioscience	TER-119	13-5921-85
Flt3	biotinylated	eBioscience	A2F10	13-1351-85
IL-7Rα	biotinylated	eBioscience	A7R34	13-1271-85
Sca-1	PE–Cy7	eBioscience	D7	25-5981-82
Sca-1	PE	eBioscience	D7	12-5981-83
Sca-1	FITC	eBioscience	D7	11-5981-85
CD117 (c-Kit)	APC-efluor780	eBioscience	ACK2	47-1172-82
CD117 (c-Kit)	APC-efluor780	eBioscience	2B8	47-1171-82
CD150	PE	eBioscience	mshad150	12-1502-82
CD150	PE	Biolegend	TC15-12F12.2	115904
CD150	PerCP-Cy5.5	Biolegend	TC15-12F12.2	115922
CD48	APC	eBioscience	HM48-1	17-0481-82
CD48	Pacific blue	Biolegend	HM48-1	103418
FLT3	PE	Invitrogen	A2F10	12-1351-82
FLT3	BV421	Biolegend	A2F10	135315
CD45	APC-efluor780	eBioscience	30-F11	47-0451-80
CD45	FITC	eBioscience	30-F11	11-0451-85
CD45	PE	Invitrogen	30-F11	12-0451-82
Ter119	APC-efluor780	eBioscience	TER-119	47-5921-82
Ter119	eFluor 450	eBioscience	TER-119	48-5921-82
CD31	PE	eBioscience	390	12-0311-82
CD31	FITC	eBioscience	390	11-0311-82
CD31	APC	eBioscience	390	17-0311-82
Gr-1	FITC	eBioscience	RB6-8C5	11-5931-85
CD11b	PE	eBioscience	M1/70	12-0112-83

CD45.1	PE-Cy7	eBioscience	A20	25-0453-82
CD45.1	PE	eBioscience	A20	12-0453-83
CD45.2	FITC	eBioscience	104	11-0454-85
CD45.2	APC	eBioscience	104	11-0454-82
Other antibodies for flow cytometry analysis				
streptavidin	PE	eBioscience		12-4317-87
streptavidin	FITC	eBioscience		11-4317-87
streptavidin	APC	Invitrogen		17-4317-82
streptavidin	Efluro 450	ebiosience		48-4317-82
Other antibodies				
anti-TNFαR1		Biolegend		55R-593
anti-TNFαR2		Biolegend		TR75-32.4
Anti-GATA2 antibody-ChIP Grade		Abcam		ab22849

Table S2. Taqman gene assays used in this study

Gene name	Assay ID
TNF-alpha	Mm00443258_m1
Ets1	Mm01175819_m1
Ets2	Mm00468973_m1
Gata2	Mm00492301_m1
β2M	Mm00437762_m1
pri-miR-126	Mm03306244_pri
pre-miR-126	Mm04335191_s1
miR-126	2228
snoRNA234	1234

Table S3. Primer sequences used for qPCR analysis

Direction	Primer name	Sequence
Forward	Mouse Gata2	5'-TAGGACAGAGAGGGGCAGGC-3'
Reverse	Mouse Gata2	5'-CTTGACCTCTGCTTCCGCCC-3'

Table S4. Murine recombinant cytokines used in this study

Name	Manufacturer	Cat #
TNFα	ThermoFisher	315-01A-5UG
IFN-γ	ThermoFisher	315-05-20UG
IL-1α	ThermoFisher	211-11A-2UG
IL-4	ThermoFisher	214-14-5UG
IL-10	ThermoFisher	210-10-2UG
IL-13	ThermoFisher	210-13-2UG
IL-16	InvivoGen	rcyc-mil16-01
M-CSF	ThermoFisher	315-02-2UG
MCP-5	ThermoFisher	250-04-5UG
MIP-1α	ThermoFisher	250-09-2UG
MIP-2	ThermoFisher	250-15-5UG
RANTES	ThermoFisher	250-07-5UG
SDF-1	ThermoFisher	250-20A-2UG
TNFSF12	R&D Systems	1237-TW-025/CF
TNFSF13B	R&D Systems	8876-BF-010/CF
TNFSF6	R&D Systems	6128-SA-025/CF
Angiopoietin-2	R&D Systems	7186-AN-025/CF

Figure S1

A

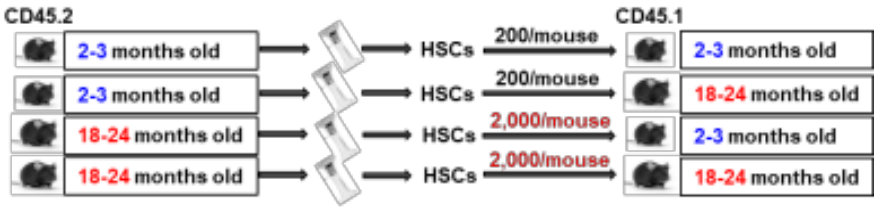

B

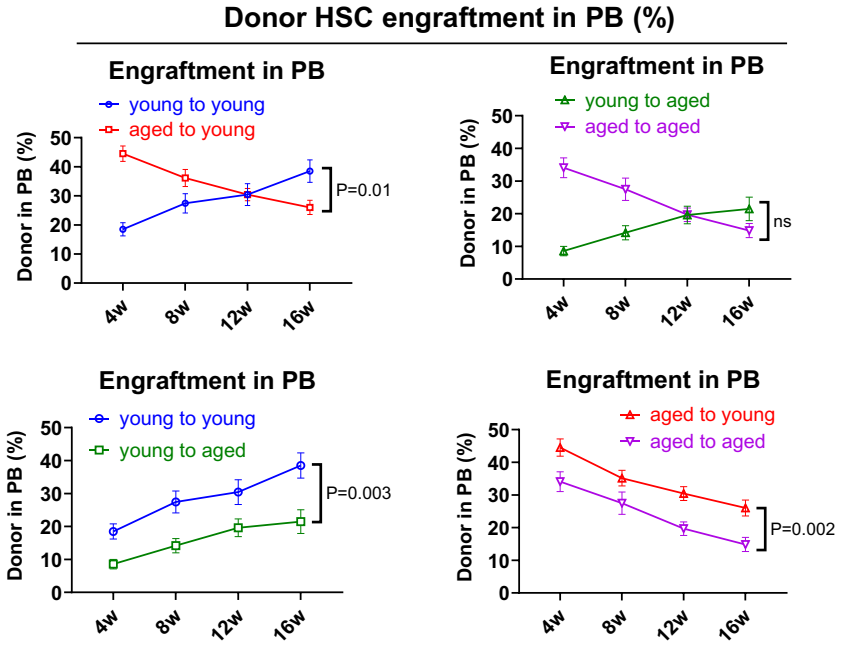

C

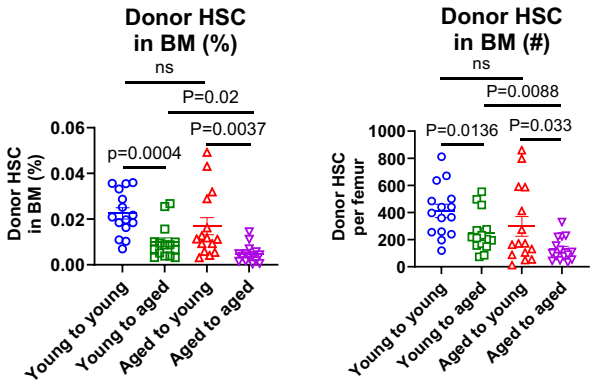

Figure S1. Aging bone marrow niche impacts HSC long-term regenerating capacity.

A-C Lineage$^-$Sca-1$^+$c-Kit$^+$FLT3$^-$CD150$^+$CD48$^-$ HSCs collected respectively from five young (2-3 months old, total 6,021 young HSCs) or five aged (18-24 months old, total 61,157 aged HSCs) mice (CD45.2) were transplanted into 15 young and 15 aged recipient mice (CD45.1; approximately 200 young HSCs/mouse or 2,000 aged HSCs/mouse; n=15 recipient mice per group; **A**), then donor HSC engraftment rates in PB of the aged recipients vs young recipients were monitored monthly by flow cytometry analysis (**B**). Donor HSC percentage (**C**, **left**) and number (**C**, **right**) in the BM of the recipient mice were measured at 16 weeks post-transplant by flow cytometry. Abbreviation: HSC: hematopoietic stem cells; BM: bone marrow. Comparison between groups was performed by two-tailed, unpaired t-test. Results shown represent mean ± SEM. Significance values: ns, not significant..

Figure S2

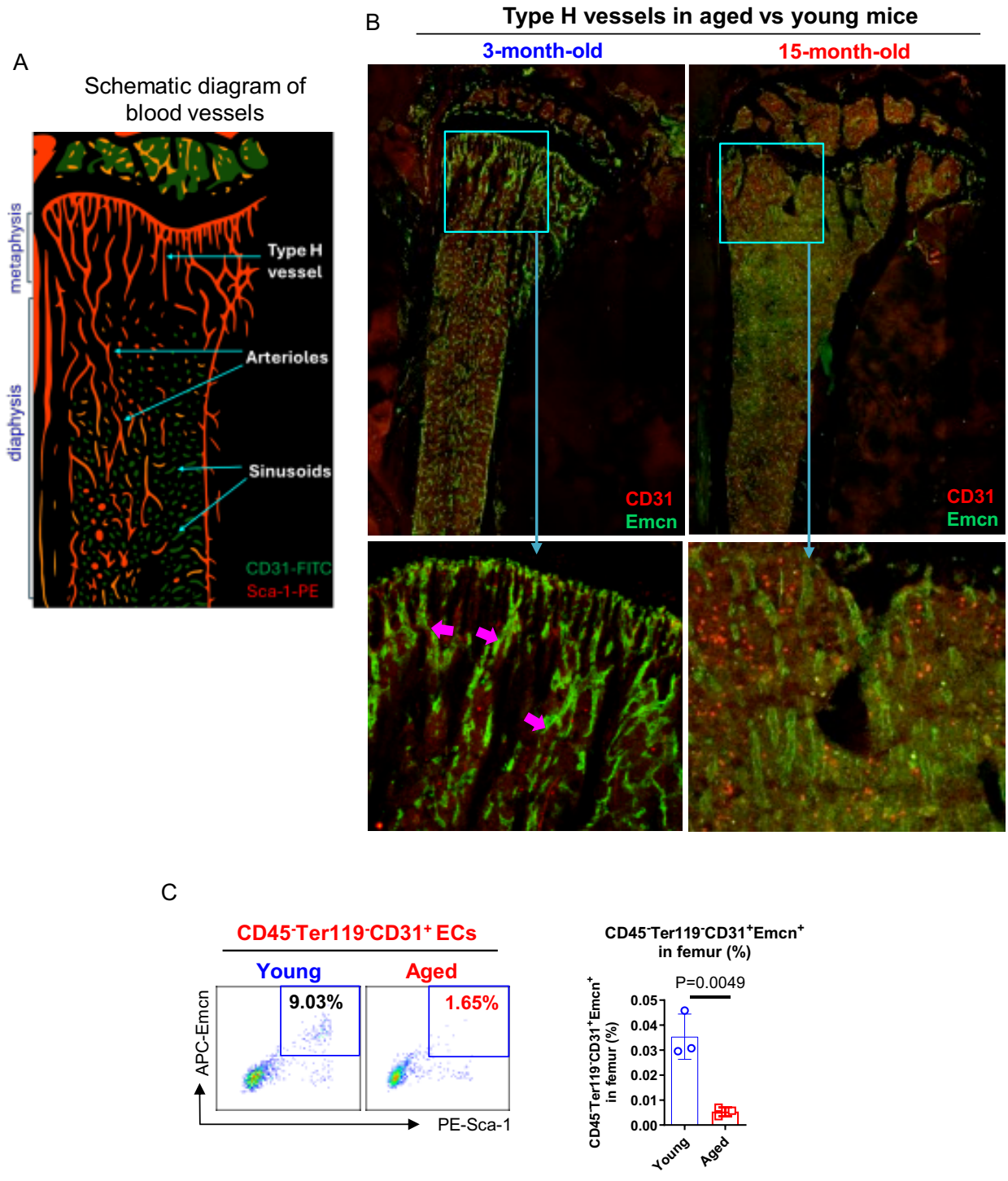
A
Schematic diagram of blood vessels
metaphysis
diaphysis
Type H vessel
Arterioles
Sinusoids
CD31-FITC
Sca-1-PE
B
Type H vessels in aged vs young mice
3-month-old
15-month-old
CD31
Emcn
CD31
Emcn
C
CD45-Ter119-CD31+ ECs
Young
Aged
9.03%
1.65%
APC-Emcn
PE-Sca-1
CD45-Ter119-CD31+Emcn+ in femur (%)
P=0.0049
0.05
0.04
0.03
0.02
0.01
0.00
Young
Aged

Figure S2. Reduced type H vessels in aged mice

A Schematic diagram of localization and structures of type H vessels, arterioles and sinusoids in long bones. $CD31^{+}Emcn^{high}$ EC-lined type H vessels locate in metaphysis of the long bone with a narrow, elongated morphology and continuous endothelial lining; $CD31^{+}Sca\text{-}1^{high}$ EC-lined arterioles locate in metaphysis and diaphysis of long bones with a narrow, elongated morphology and continuous endothelial lining; and $CD31^{+}Sca\text{-}1^{low}$ EC-lined sinusoids locate in diaphysis, are highly branched with a thin wall. **B** CD31 (PE) and Endomucin (Emcn, FITC) immunofluorescence staining of $CD31^{+}Emcn^{high}$ EC-lined type H vessels in tibias from 3 and 15 months old mice, assessed by immunofluorescent staining and 3D confocal imaging. Purple arrows indicate $CD31^{+}Emcn^{high}$ EC-lined type H vessels. One of the three independent experiments with similar results is shown. **C** Representative plots and combined results (n=3 mice per group) of flow cytometry analysis of Emcn and Sca-1 expression in $CD45^{-}Ter119^{-}CD31^{+}$ BM ECs from young (2-3 months old) and aged (15-20 months old) mice. Comparison between groups was performed by two-tailed, unpaired t-test. Results shown represent mean ± SD.

Figure S3

Quantification of arterioles in the bone marrow niche

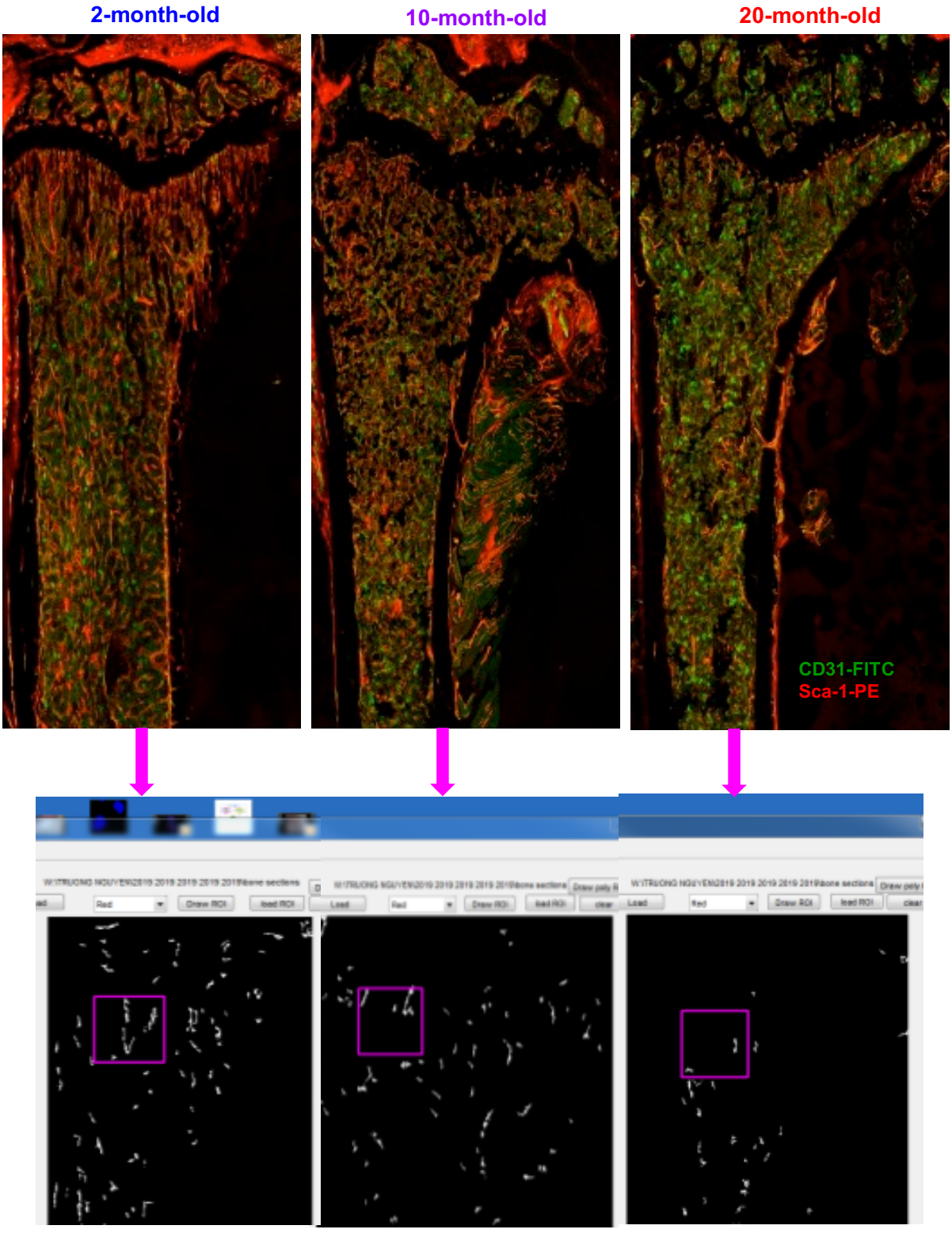

Figure S3. Quantification of arterioles in bone marrow niche

Quantification of $CD31^{+}Sca\text{-}1^{high}$ EC-lined arterioles in tibias from 2, 10 and 20 months old mice, relative to Figure 2A-B. To identify blood vessels, connected objects of Sca-1-PE signal with a threshold of 80 as a cutoff were identified and those with fewer than 15 pixels were removed to reduce noise using MATLAB's bwareafilt function. The image was then morphologically closed with a 1.0-pixel filter using MATLAB's imclose function to close any holes. The perimeter:area ratio was calculated for each object; objects with a ratio of less than 0.7 were removed using MATLAB's bwconncomp and bwperim functions. Finally, the fractions of pixels (i.e., arbitrary unit) that registered as positive for blood vessels within three representative hand-drawn regions of interest were reported as the quantification of arterioles. Purple square indicates one of the representative hand-drawn regions to quantify arterioles.

Figure S4

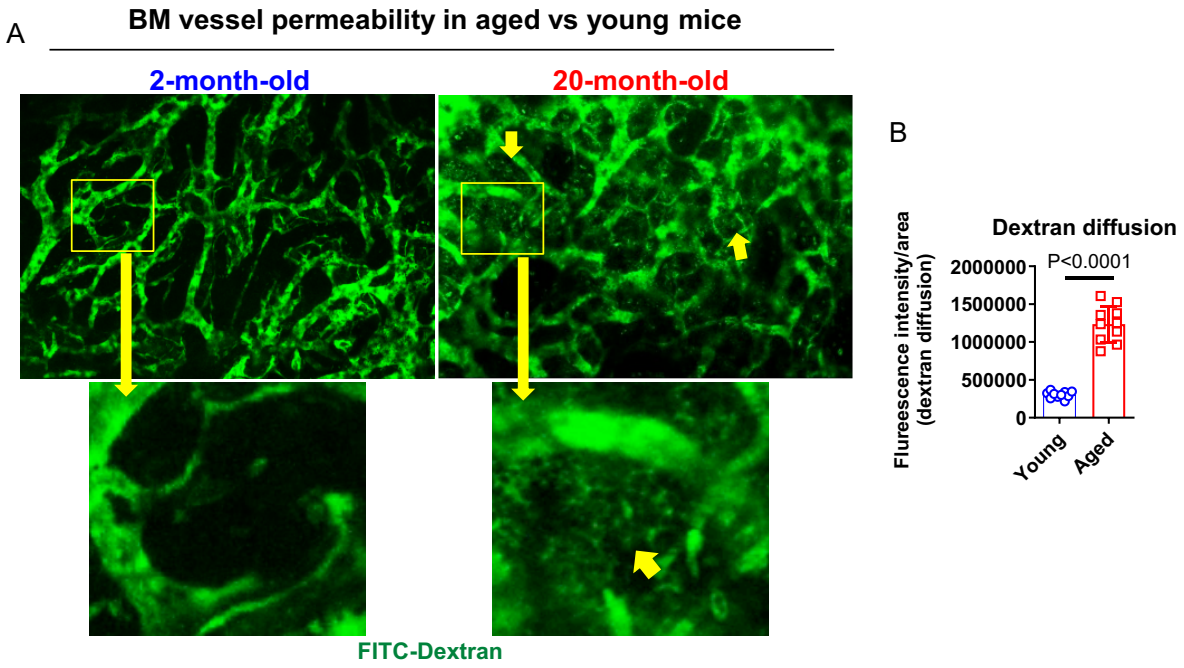

Figure S4. Increased BM vessel permeability in aged mice

A-B Representative images (A) and quantification (B) of dextran leakiness out of calvarial vessels in young (2 months old) and aged (20 months old) mice (FITC-150 kDa dextran, green), assessed at 30 minutes post dextran administration using intravital confocal microscopy. Vascular permeability quantified by the dextran outside of the vessels using Zen Lite 3.3 software (Zeiss). For each group of mice, 10 random regions of interest (ROIs) were selected outside the vessel wall using a fixed-size square box. The green fluorescence intensity within each ROI, after subtracting the background fluorescence, was used to assess extravascular dextran leakage. Yellow arrows indicate representative regions of leakiness (i.e., diffuse dextran staining) observed mainly outside the vessels in the aged mice. One of three independent experiments with similar

results is shown. Comparison between groups was performed by two-tailed, unpaired t-test. Results shown represent mean ± SD.

Figure S5

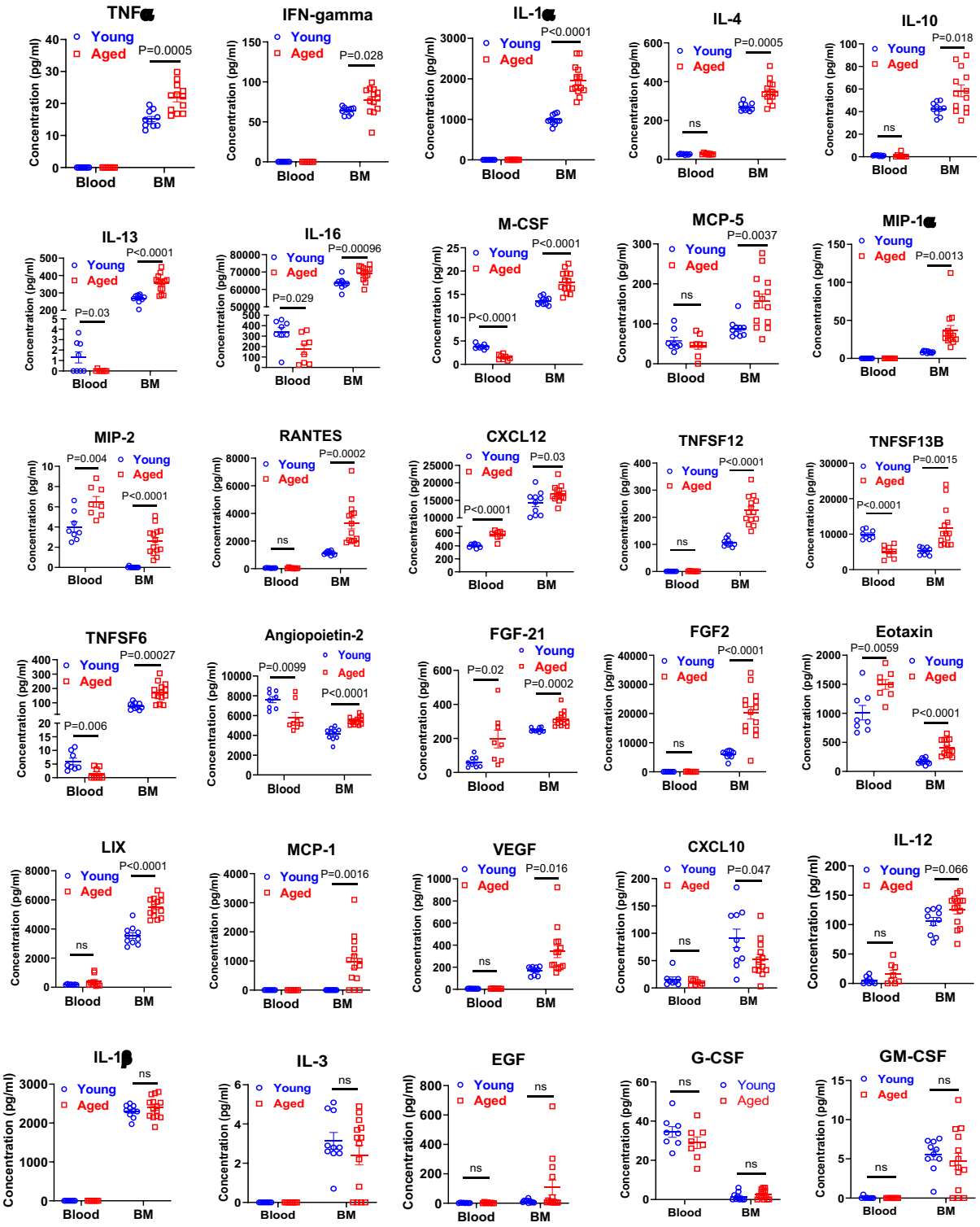
TNFα
IFN-gamma
IL-1α
IL-4
IL-10
IL-13
IL-16
M-CSF
MCP-5
MIP-1α
MIP-2
RANTES
CXCL12
TNFSF12
TNFSF13B
TNFSF6
Angiopoietin-2
FGF-21
FGF2
Eotaxin
LIX
MCP-1
VEGF
CXCL10
IL-12
IL-1β
IL-3
EGF
G-CSF
GM-CSF
Young
Aged
Concentration (pg/ml)
Blood
BM
P=0.0005
P=0.028
P<0.0001
P=0.0005
P=0.018
P<0.0001
P=0.03
P=0.029
P=0.00096
P<0.0001
P<0.0001
P=0.0037
P=0.0013
P=0.004
P<0.0001
P=0.0002
P=0.03
P<0.0001
P<0.0001
P=0.0015
P<0.0001
P=0.00027
P=0.006
P=0.0099
P<0.0001
P=0.02
P=0.0002
P<0.0001
P=0.0059
P<0.0001
P<0.0001
P=0.0016
P=0.016
P=0.047
P=0.066
ns

Figure S5. Altered cytokine levels in aged vs young mice

Blood (n=8 mice for each group) and BM (n=10 young mice; n=14 aged mice) cytokine levels in young (2-3 months old) and aged (18-24 months old) wt mice were measured by Luminex assay. Abbreviation: BM: bone marrow; vs: versus; wt: wild-type; ECs: endothelial cells; Ang-2: Angiopoietin-2. Comparison between groups was performed by two-tailed, unpaired t-test. Results shown represent mean ± SEM. Significance values: ns, not significant.

Figure S6

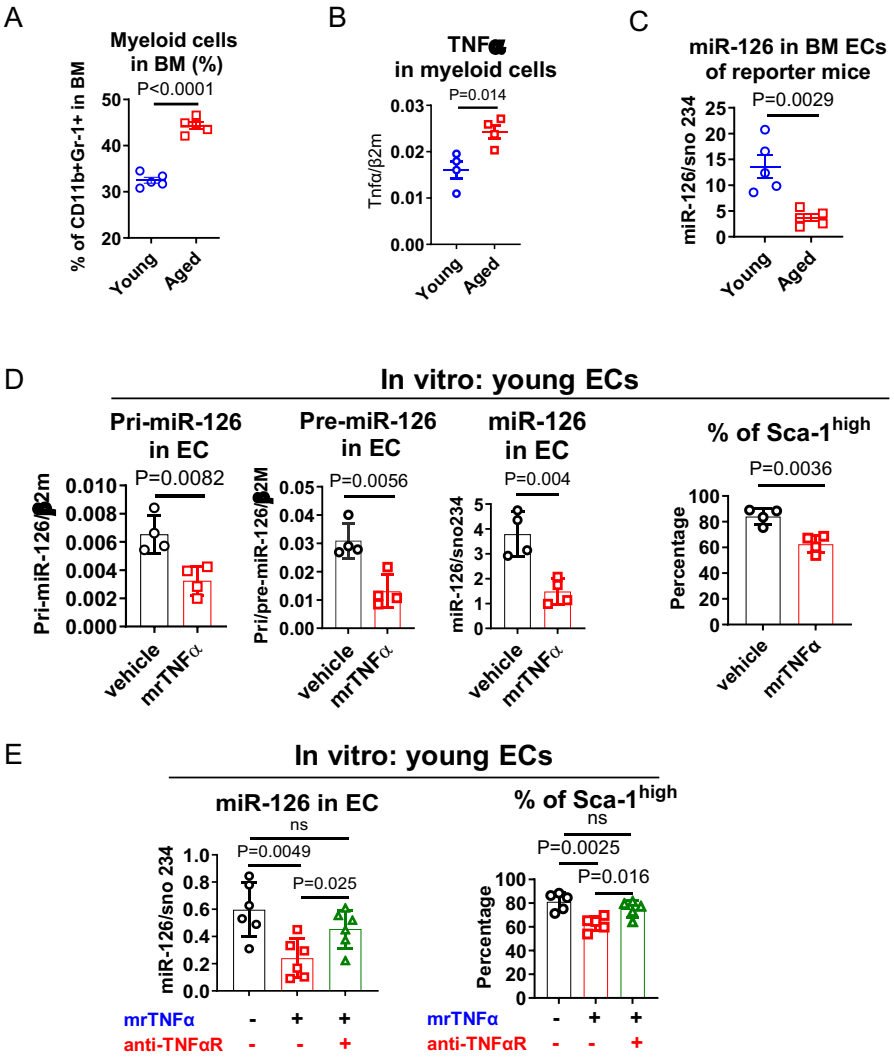
A
Myeloid cells in BM (%)
P<0.0001
% of CD11b+Gr-1+ in BM
Young
Aged
B
TNFα in myeloid cells
P=0.014
Tnfα/β2m
C
miR-126 in BM ECs of reporter mice
P=0.0029
miR-126/sno 234
D
In vitro: young ECs
Pri-miR-126 in EC
P=0.0082
Pre-miR-126 in EC
P=0.0056
miR-126 in EC
P=0.004
miR-126/sno234
% of Sca-1high
P=0.0036
Percentage
vehicle
mrTNFα
E
In vitro: young ECs
miR-126 in EC
ns
P=0.0049
P=0.025
miR-126/sno 234
% of Sca-1high
ns
P=0.0025
P=0.016
Percentage
mrTNFα
anti-TNFαR

Figure S6. TNFα induced miR-126 downregulation in ECs

A Percentages of $CD11b^{+}Gr\text{-}1^{+}$ myeloid cell population in BM from aged vs young mice (n=5 per group). **B** Levels of TNFα mRNA in myeloid cells from aged vs young mice analyzed by Q-RT-PCR (n=4 per group). **C** miR-126 levels in BM ECs from young (2-3 months old, n=5 mice) and aged (18-24 months old, n=5 mice) double fluorescent reporter mice [*Tie2-CreER/TdTomato/Tg(Ly6a-GFP)*], analyzed by Q-RT-PCR. **D** Pri, pre and mature miR-126 levels in BM ECs isolated from young mice (2-3 months old; n=4 mice) and treated in vitro with vehicle PBS or mrTNFα (1ng/ml) for 8 hours, analyzed by Q-RT-PCR (**left**) and $Sca\text{-}1^{high}$ and $Sca\text{-}1^{low}$ subpopulations in young BM ECs treated with vehicle PBS or mrTNFα (1ng/ml) for 96 hours, analyzed by flow cytometry (**right**). **E** miR-126 levels in BM ECs exposed to vehicle PBS, mrTNFα (1ng/ml), or mrTNFα+anti-TNFαR1/R2 (1μg/ml) for 8 hours, analyzed by Q-RT-PCR (**left**) and $Sca\text{-}1^{high}$ and $Sca\text{-}1^{low}$ subpopulations in BM ECs exposed to vehicle PBS, mrTNFα (1ng/ml), or mrTNFα+anti-TNFαR1/R2 (1μg/ml) for 96 hours, analyzed by flow cytometry (**right**). Abbreviation: ECs: endothelial cells; BM: bone marrow; wt: wild-type; pri: primary; pre: precursor; mr: murine recombinant; TNFαR1/R2: TNFα receptor type 1 and 2; anti-TNFαR1/R2: TNFαR1 and TNFαR2 blocking antibodies. Comparison between groups was performed by two-tailed, unpaired t-test. Results shown represent mean ± SD. Significance values: ns, not significant.

Figure S7

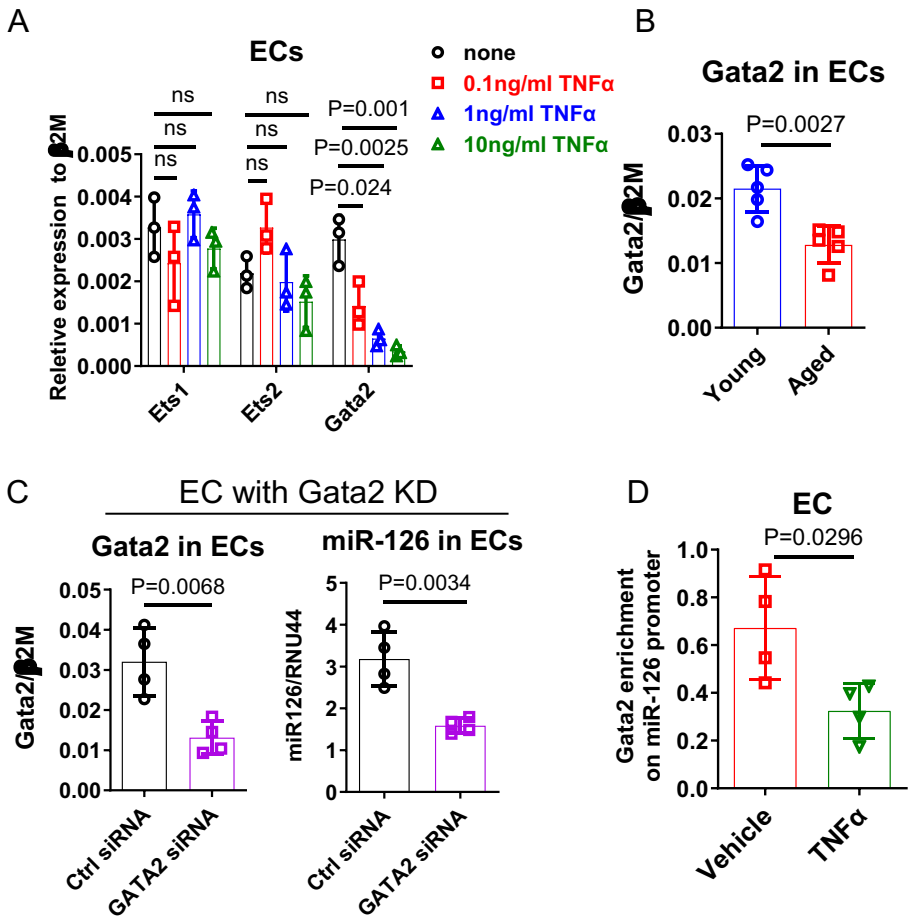

Figure S7. Gata2 mediates TNFα-induced miR-126 downregulation in ECs. **A** Ets1, Ets2 and Gata2 mRNA in BM ECs treated with 0.1, 1 and 10 ng/ml mrTNFα for 8 hours, analyzed by Q-RT-PCR (n=3 samples per group). **B** Gata2 mRNA in BM ECs from young (2-3 months old) and aged (18-24 months old) mice (n=5 mice each), analyzed by Q-RT-PCR. **C** Gata2 mRNA and miR-126 levels in mouse ECs transduced with Gata2 siRNA or control siRNA, measured by Q-RT-PCR (n=4). **D** Enrichment of GATA2 on the EGFL7/miR-126 promoter in ECs treated with mrTNFα (1ng/ml) or vehicle PBS for 24 hours, analyzed by ChIP assay using anti-GATA2 antibody followed by quantitative-PCR using primers for the miR-126 promotor region flanking the GATA2 binding site. Abbreviation: ECs: endothelial cells; mr: murine recombinant; ChIP:

chromatin immunoprecipitation. Results represent mean ± SD. Significance values: ns, not significant.

Figure S8

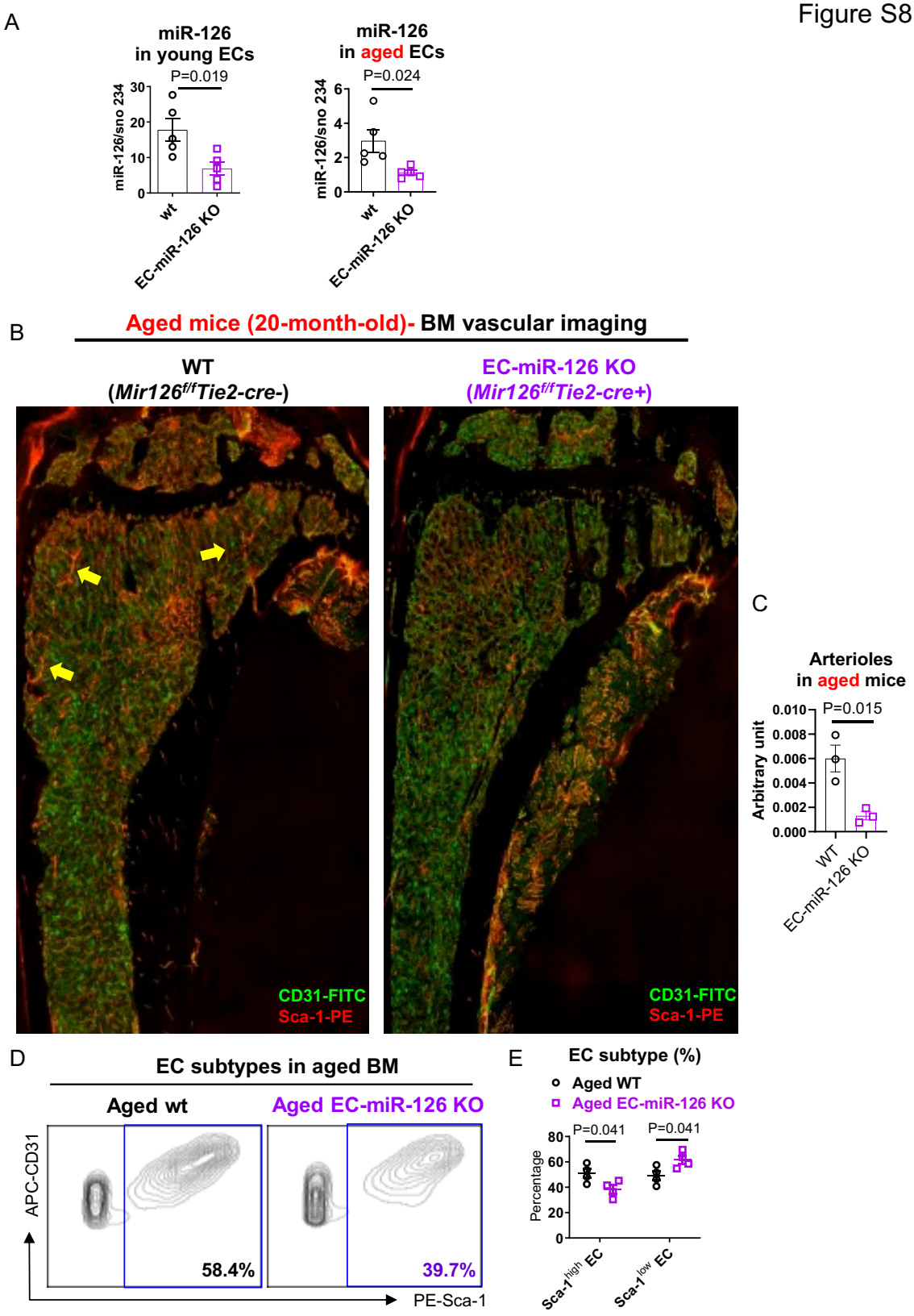
A
miR-126
in young ECs
P=0.019
miR-126/sno 234
wt
EC-miR-126 KO
miR-126
in aged ECs
P=0.024
B
Aged mice (20-month-old)- BM vascular imaging
WT
(Mir126f/fTie2-cre-)
EC-miR-126 KO
(Mir126f/fTie2-cre+)
CD31-FITC
Sca-1-PE
C
Arterioles
in aged mice
P=0.015
Arbitrary unit
D
EC subtypes in aged BM
Aged wt
Aged EC-miR-126 KO
APC-CD31
PE-Sca-1
58.4%
39.7%
E
EC subtype (%)
Aged WT
Aged EC-miR-126 KO
P=0.041
P=0.041
Percentage
Sca-1high EC
Sca-1low EC

Figure S8. Reduced CD31^{+}Sca-1^{high} EC-lined arterioles in aged EC-miR-126 KO (*Mir126$^{f/f}$Tie2-cre*+) vs wt (*Mir126$^{f/f}$Tie2-cre*-) mice

A miR-126 levels in BM ECs from young (2-3 months old, n=5 mice per group) and aged (18-24 months old, n=5 mice per group) *Mir126$^{f/f}$Tie2-cre*- (WT) and *Mir126$^{f/f}$Tie2-cre*+ (EC-miR-126 KO) mice, analyzed by Q-RT-PCR. **B-C** CD31-FITC and Sca-1-PE immunofluorescence staining and 3D confocal imaging (**B**) and quantification (**C**) of CD31^{+}Sca-1^{high} EC-lined vessels (i.e., arterioles) in tibias from 20 months old *Mir126$^{f/f}$Tie2-cre*- (WT) and *Mir126$^{f/f}$Tie2-cre*+ (EC-miR-126 KO) mice. One of the three independent experiments with similar results is shown. Yellow arrows indicate CD31^{+}Sca-1^{high} EC-lined vessels. **D-E** Representative plots (**D**) and combined results (**E**) of CD31^{+}Sca-1^{high} and CD31^{+}Sca-1^{low} EC subpopulations in femurs from 20 months old *Mir126$^{f/f}$Tie2-cre*- (WT) and *Mir126$^{f/f}$Tie2-cre*+ (EC-miR-126 KO) mice, analyzed by flow cytometry (n=4 mice per group). Abbreviation: BM: bone marrow; ECs: endothelial cells; wt: wild-type. Comparison between groups was performed by two-tailed, unpaired t-test. Results shown represent mean ± SEM.

Figure S9

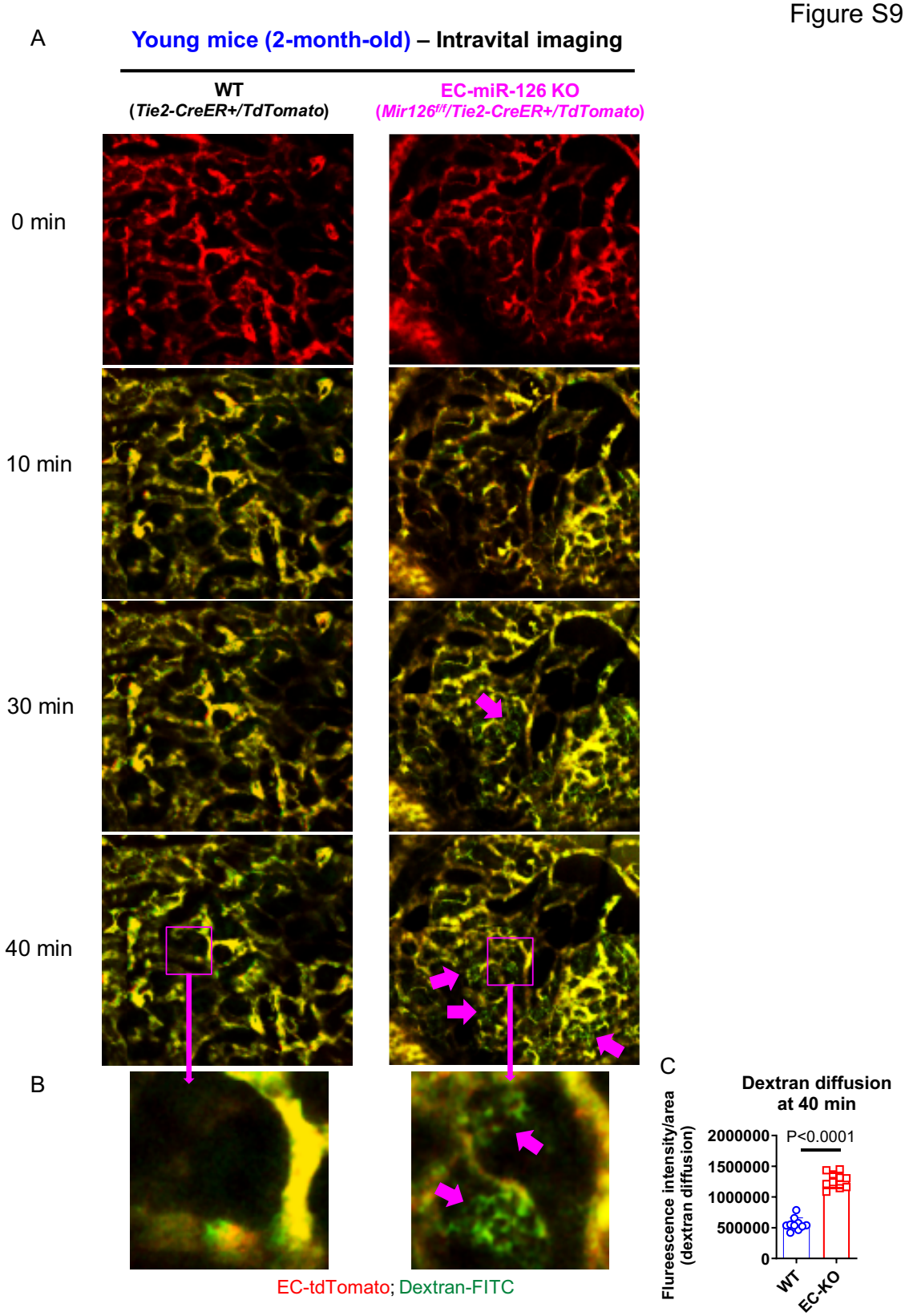
A
Young mice (2-month-old) – Intravital imaging
WT
(Tie2-CreER+/TdTomato)
EC-miR-126 KO
(Mir126f/f/Tie2-CreER+/TdTomato)
0 min
10 min
30 min
40 min
B
EC-tdTomato; Dextran-FITC
C
Dextran diffusion
at 40 min
Fluorescence intensity/area
(dextran diffusion)
2000000
1500000
1000000
500000
0
P<0.0001
WT
EC-KO

Figure S9. Increased BM vessel permeability in young *Mir126$^{f/f}$Tie2-cre*+ vs *Mir126$^{f/f}$Tie2-cre*- mice

A-C Vessel permeability as shown by dextran leakiness out of calvarial vessels in 2 months old *Tie2-CreER+/TdTomato* (WT, tamoxifen-induced CD31-TdTomato^{+}) and *Mir126$^{f/f}$/Tie2-CreER+/TdTomato* (tamoxifen-induced EC-miR-126 KO and CD31-TdTomato^{+}) mice, assessed at 0, 10, 30 and 40 minutes (**A-B**) and quantification of dextran leakage outside of vessels at 40 minutes (**C**) post dextran administration (FITC-150 kDa dextran, green) using intravital confocal microscopy. One of the three independent experiments with similar results is shown. Dextran leakage was quantified using Zen Lite 3.3 software (Zeiss). For each group of mice, 10 random regions of interest (ROIs) were selected outside the vessel wall using a fixed-size square box. The green fluorescence intensity within each ROI, after subtracting the background fluorescence, was used to assess extravascular dextran leakage. Purple arrows indicate representative regions of leakiness (i.e., diffuse dextran staining) observed mainly outside the vessels of *Mir126$^{f/f}$/Tie2-CreER+/TdTomato* mice. Abbreviation: BM: bone marrow; vs: versus; WT: wild type; EC: endothelial cell; KO: knock out; min: minutes.

Figure S10

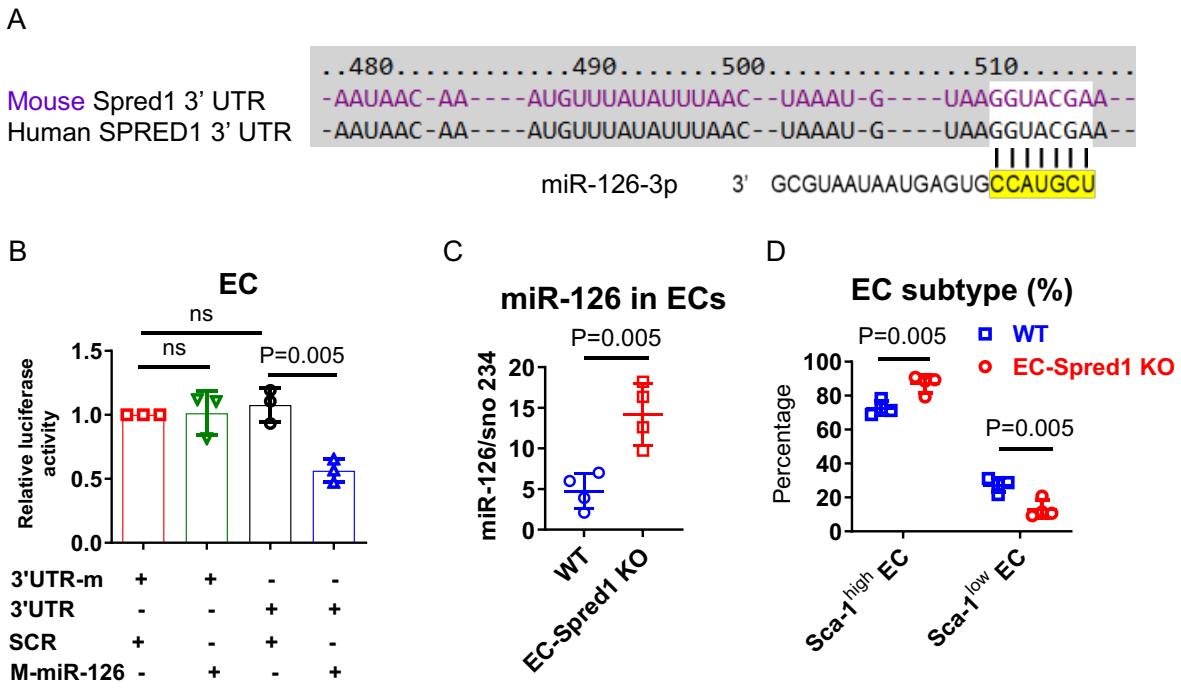

Figure S10. MiR-126 regulates Spred1 expression and EC-Spred1 KO functionally represents EC-miR-126 overexpression

A Sequence alignment of miR-126 with Spred-1 3' untranslated regions (UTRs) from mouse and human. **B** Luciferase assay using Spred1 3' UTR. The Spred1 3' UTR and 3' UTR with mutations engineered in the region complementary to the miR-126 seed region (GGTACGA to TTGGAAG; 3' UTR-m) was inserted into the psiCHECK-2 vector (Promega). Mouse ECs (C166, from ATCC) were transfected with the Spred1 3' UTR or 3' UTR-m plasmids, in the presence or absence of miR-126 mimic (M-miR-126, 2μM) or scrambled RNA (SCR) and firefly luciferase reporter activity was normalized with renilla luciferase as internal control (red: 3' UTR-m + SCR; green: 3' UTR-m + M-miR-126; black: 3' UTR + SCR; blue: 3' UTR + M-miR-126; n=3). **C** miR-126 levels in BM ECs from *Spred1$^{f/f}$Tie2-cre*+ (EC-Spred1 KO) vs *Spred1$^{f/f}$Tie2-cre*- (WT) mice, analyzed by Q-

RT-PCR (n=4 mice per group). **D** $CD31^{+}Sca\text{-}1^{high}$ and $CD31^{+}Sca\text{-}1^{low}$ EC subpopulations in femurs from *Spred1$^{f/f}$Tie2-cre*+ (EC-Spred1 KO) vs *Spred1$^{f/f}$Tie2-cre*- (WT) mice, analyzed by flow cytometry (n=4 mice per group). Abbreviation: vs: versus; ECs: endothelial cells; wt: wild-type. Comparison between groups was performed by two-tailed, unpaired t-test. Results shown represent mean ± SD. Significance values: ns, not significant.

,

Figure S11

A

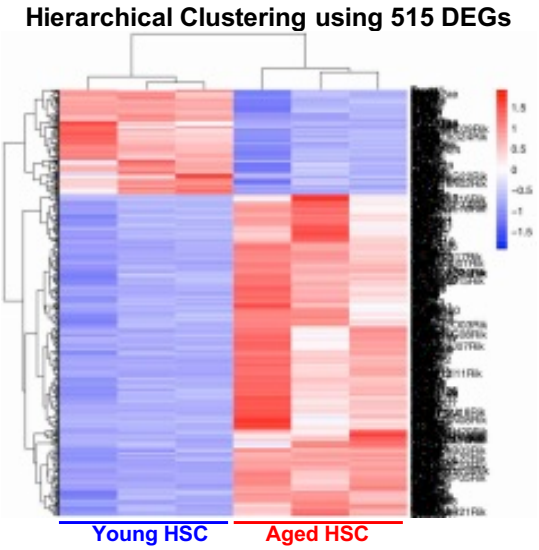

B

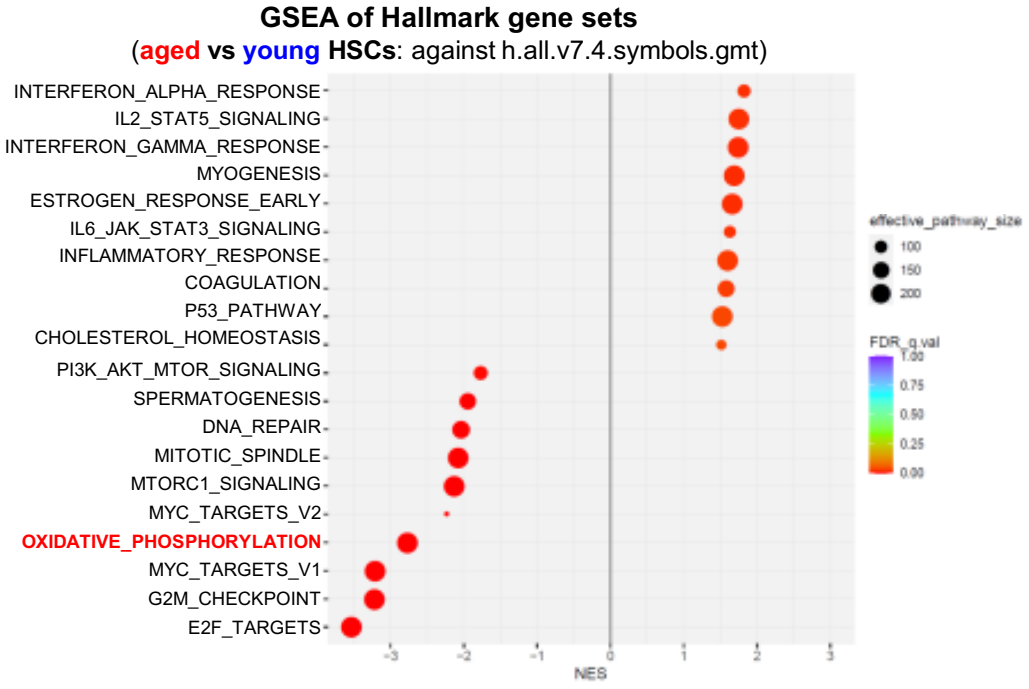

Figure S11. RNA-Seq analysis reveals DEGs and top 10 up or down-regulated pathways in HSCs affected by aging

A Heat map showing levels of DEGs in aged vs young HSCs by RNA-seq using lineage-Sca-1+c-Kit+CD150+CD48- HSCs from young or aged mice (n=3 young HSC samples, pooled from 30 of 2-3 months old mice; n=3 aged HSC samples, pooled from 4 of 18-24 months old mice). **B** GSEA of hallmark gene sets showing top 10 up- or down-regulated pathways in aged vs young HSCs. Abbreviation: HSCs: hematopoietic stem cells; DEGs: differentially expressed genes; vs: versus; GSEA: gene set enrichment analysis.

Figure S12

A

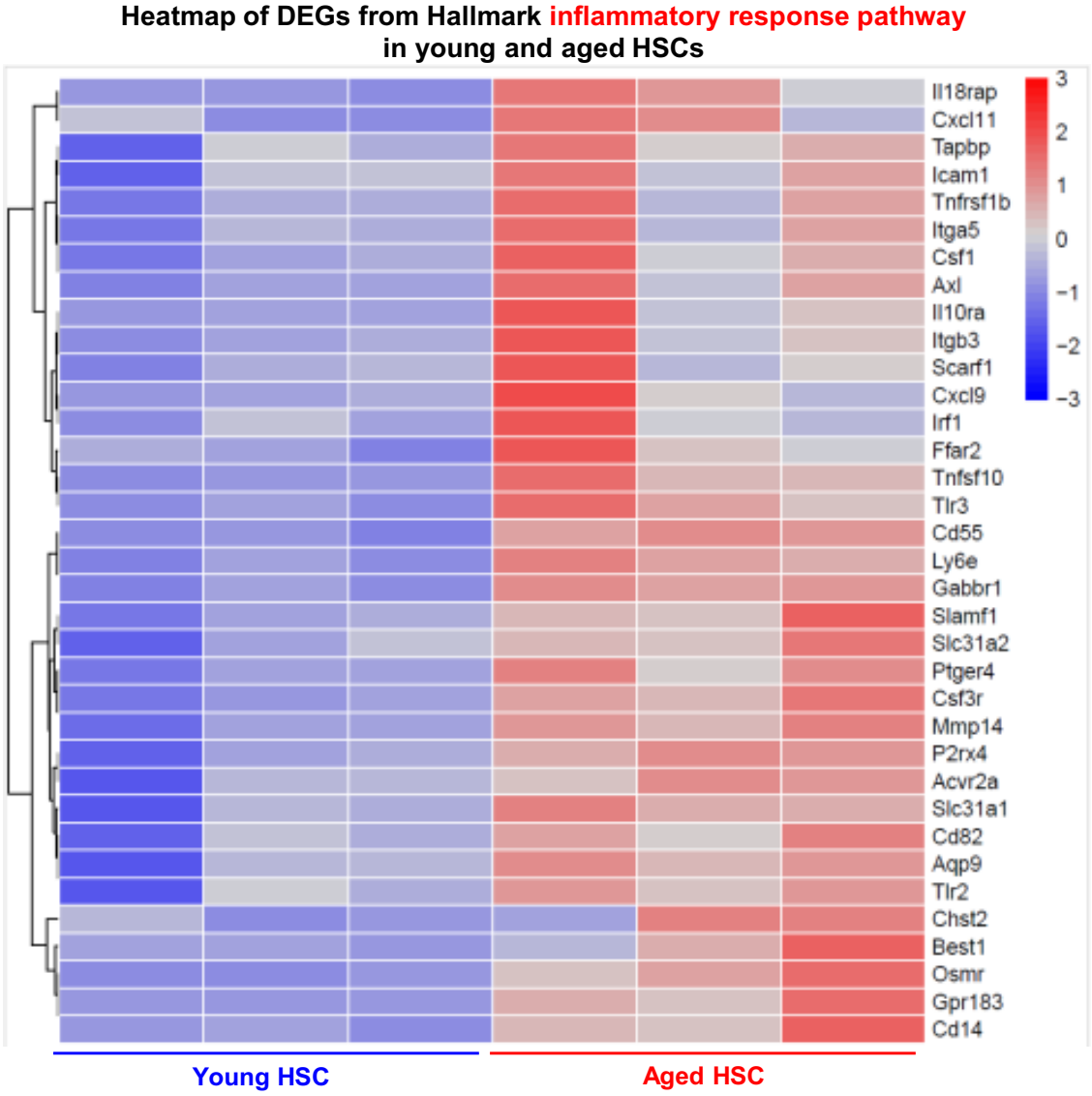

B

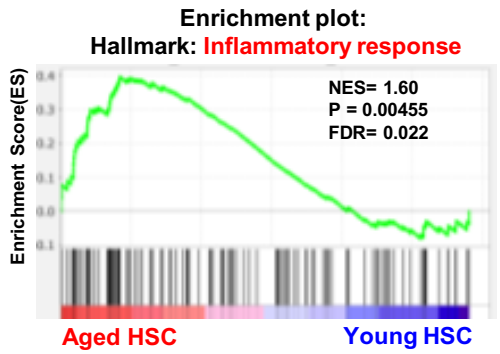

Figure S12. RNA-Seq analysis reveals DEGs and gene set enrichment plot from inflammatory response pathway in aged vs young HSCs

A Heat map showing levels of DEGs from inflammatory response pathway in HSCs selected from aged vs young mice, by RNA-seq analysis. **B** Enrichment plot of inflammatory response pathway gene sets in aged vs young HSCs. Abbreviation: DEGs: differentially expressed genes; HSC: Lineage-Sca-1+c-Kit+CD150+CD48- hematopoietic stem cells; NES: normalized enrichment score; FDR: false discovery rate.

Figure S13

A

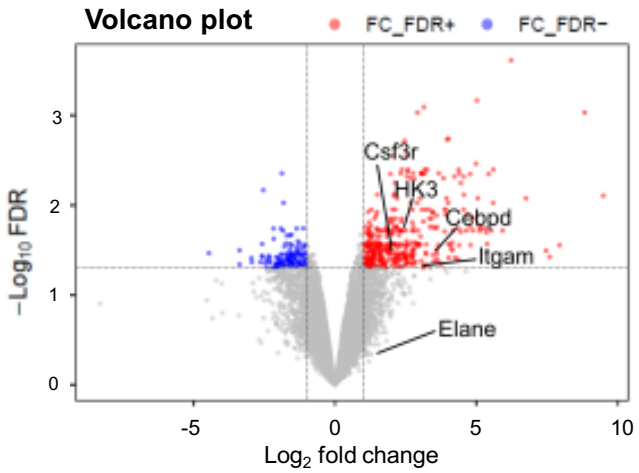

B

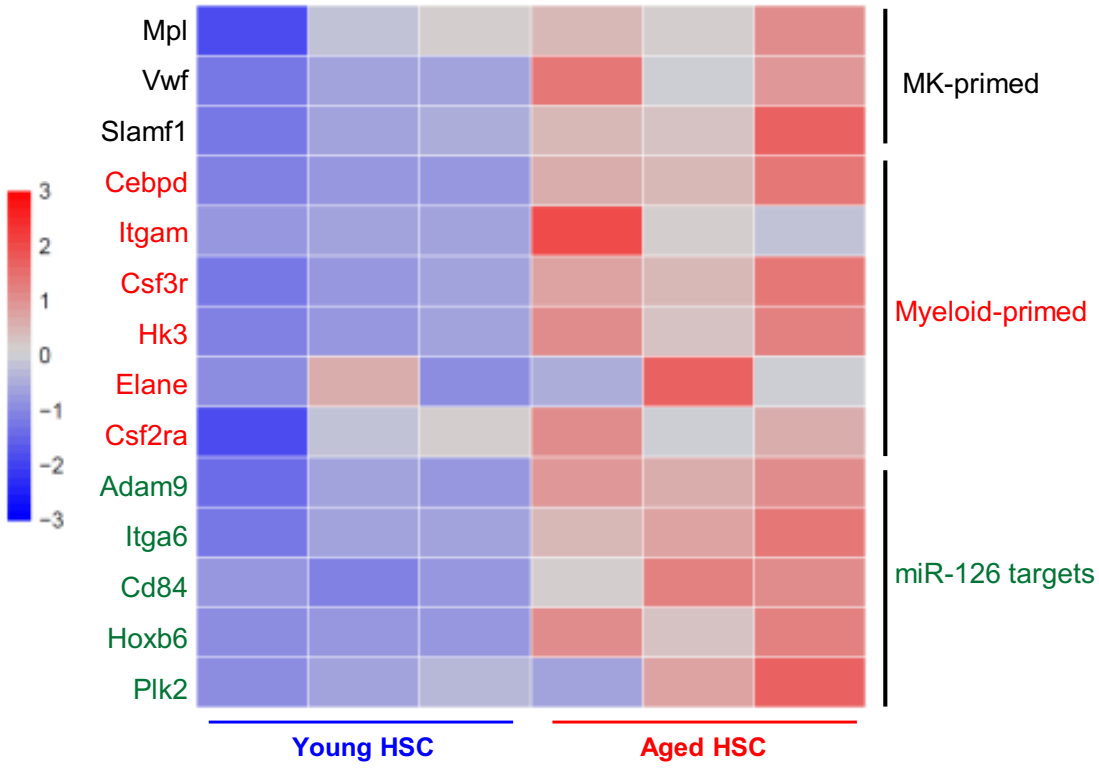

Figure S13. RNA-Seq analysis reveals DEGs relative to megakaryocyte and myeloid differentiation and miR-126 targets in aged vs young HSCs

A Volcano plot illustrating gene expression levels from RNA-seq analysis of aged vs young HSCs. Genes upregulated and downregulated in aged HSCs are shown in red and blue, respectively. **B** Heat map showing levels of megakaryocyte and myeloid marker genes and miR-126 target genes in aged vs young HSCs. Abbreviation: DEGs: differentially expressed genes; HSC: Lineage-Sca-1+c-Kit+CD150+CD48- hematopoietic stem cells; MK: megakaryocyte.

Figure S14

A

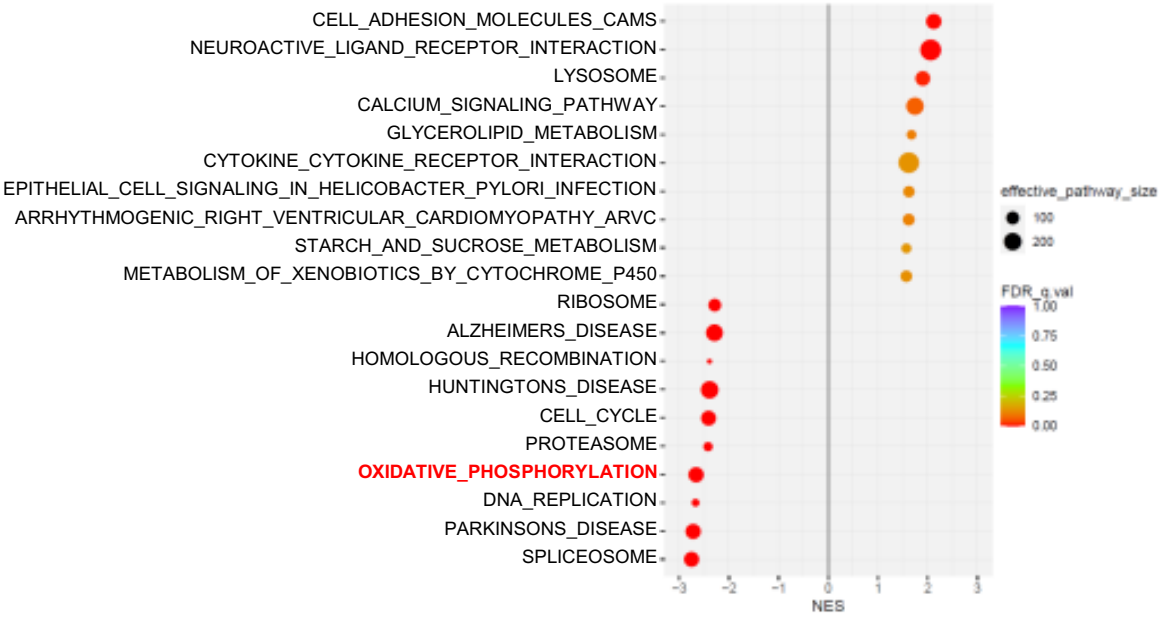

B

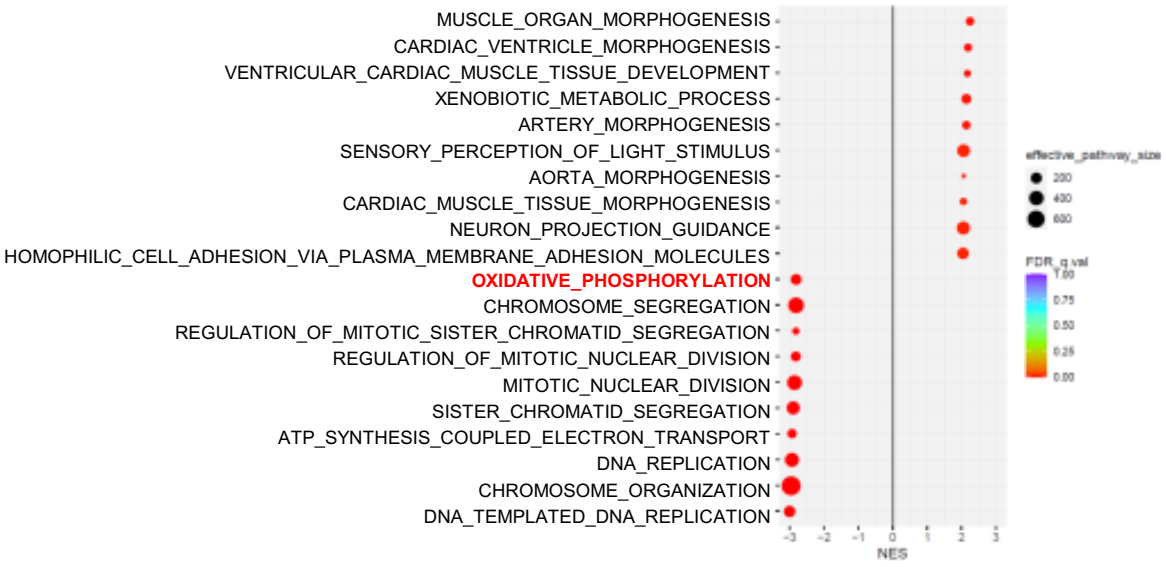

Figure S14. GSEA of KEGG and GO gene sets from young and aged HSCs by RNA-seq

a-b GSEA of KEGG (**a**) and GO (**b**) gene sets showing top 10 up- or down-regulated pathways in HSCs from aged vs young mice. Abbreviation: GSEA: gene set enrichment analysis; HSCs: Lineage-Sca-1+c-Kit+CD150+CD48- hematopoietic stem cells.

Figure S15

A

Heatmap of DEGs from Hallmark oxidative phosphorylation pathway in young and aged HSCs

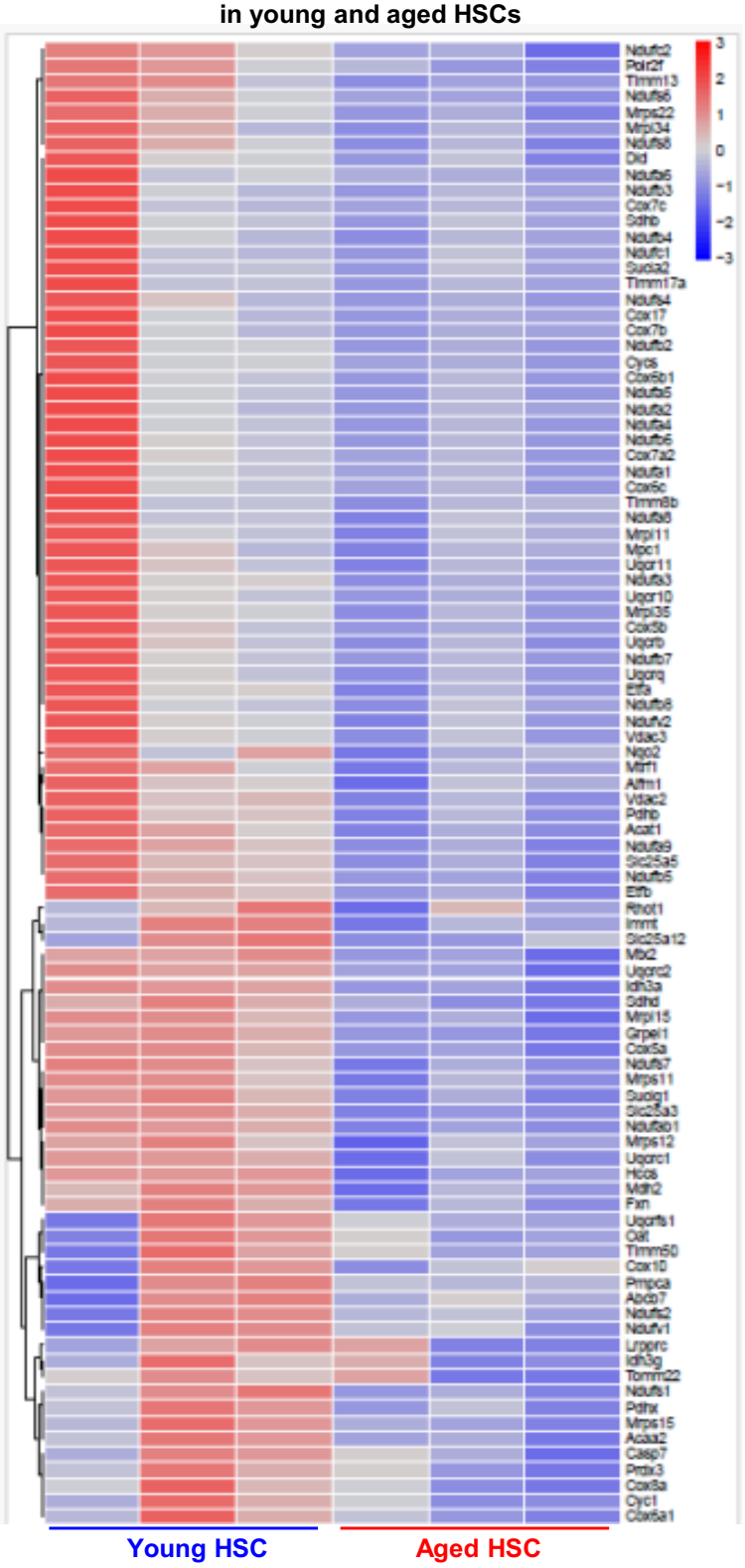

B

Enrichment plot: Hallmark: Oxidative phosphorylation

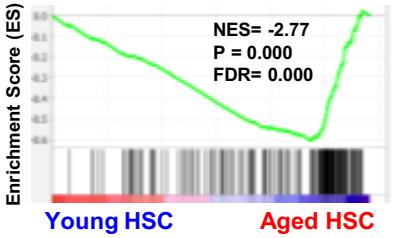

Figure S15. RNA-Seq analysis reveals DEGs from oxidative phosphorylation pathway in aged vs young HSCs

A Heat map showing levels of DEGs from oxidative phosphorylation pathway in HSCs selected from aged vs young mice, by RNA-seq analysis. **B** Enrichment plot of hallmark gene sets involved in oxidative phosphorylation from aged vs young HSCs. Abbreviation: DEGs: differentially expressed genes; vs: versus; HSC: Lineage-Sca-1+c-Kit+CD150+CD48- hematopoietic stem cells; NES: normalized enrichment score; FDR: false discovery rate.

Figure S16

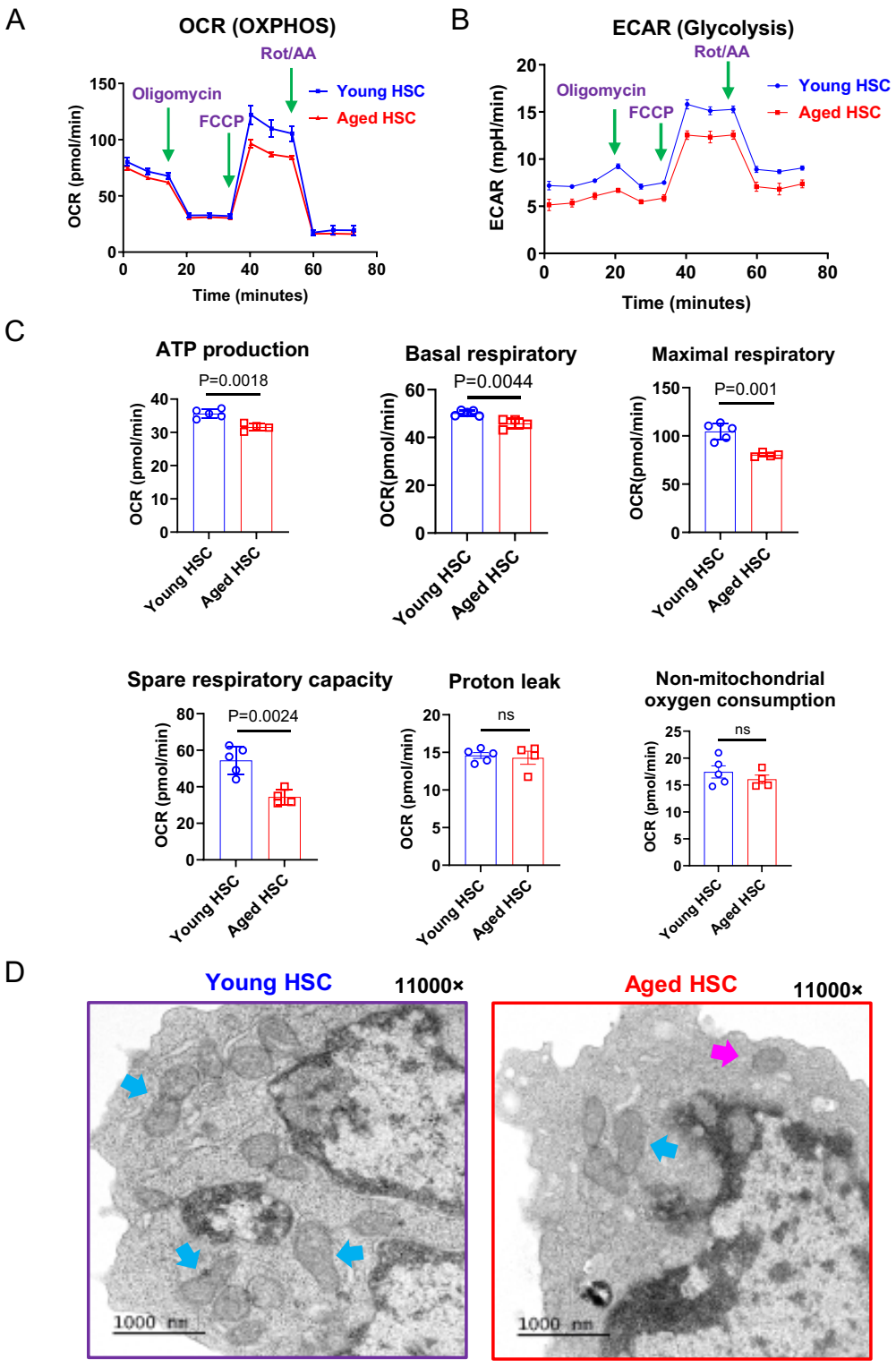
A
OCR (OXPHOS)
Rot/AA
Oligomycin
FCCP
Young HSC
Aged HSC
OCR (pmol/min)
Time (minutes)
B
ECAR (Glycolysis)
Rot/AA
Oligomycin
FCCP
Young HSC
Aged HSC
ECAR (mpH/min)
Time (minutes)
C
ATP production
P=0.0018
OCR (pmol/min)
Young HSC
Aged HSC
Basal respiratory
P=0.0044
OCR(pmol/min)
Young HSC
Aged HSC
Maximal respiratory
P=0.001
OCR(pmol/min)
Young HSC
Aged HSC
Spare respiratory capacity
P=0.0024
OCR (pmol/min)
Young HSC
Aged HSC
Proton leak
ns
OCR (pmol/min)
Young HSC
Aged HSC
Non-mitochondrial oxygen consumption
ns
OCR (pmol/min)
Young HSC
Aged HSC
D
Young HSC
11000×
1000 nm
Aged HSC
11000×
1000 nm

Figure S16. Seahorse assay and mitochondria imaging of young and aged HSCs

A-C Levels of OCR indicating OXPHOS (**A**) and ECAR indicating glycolysis (**B**) and ATP production, basal respiratory, maximal respiratory, spare respiratory capacity, proton leak, and non-mitochondrial oxygen consumption (**C**) in aged vs young HSCs, analyzed by seahorse assays. **D** Mitochondria morphology (blue arrows indicate mitochondrial fusion; purple arrow indicates mitochondrial fission) in aged vs young HSCs, analyzed by electron microscope. Abbreviation: HSC: Lineage-Sca-1+c-Kit+CD150+CD48- hematopoietic stem cells; OCR: oxygen consumption rate; OXPHOS: oxidative phosphorylation; ECAR: extracellular acidification rate; FCCP: carbonyl cyanide-4 (trifluoromethoxy) phenylhydrazone; Rot/AA: rotenone and antimycin A. Comparison between groups was performed by two-tailed, unpaired t-test. Results shown represent mean ± SD. Significance values: ns, not significant.

Figure S17

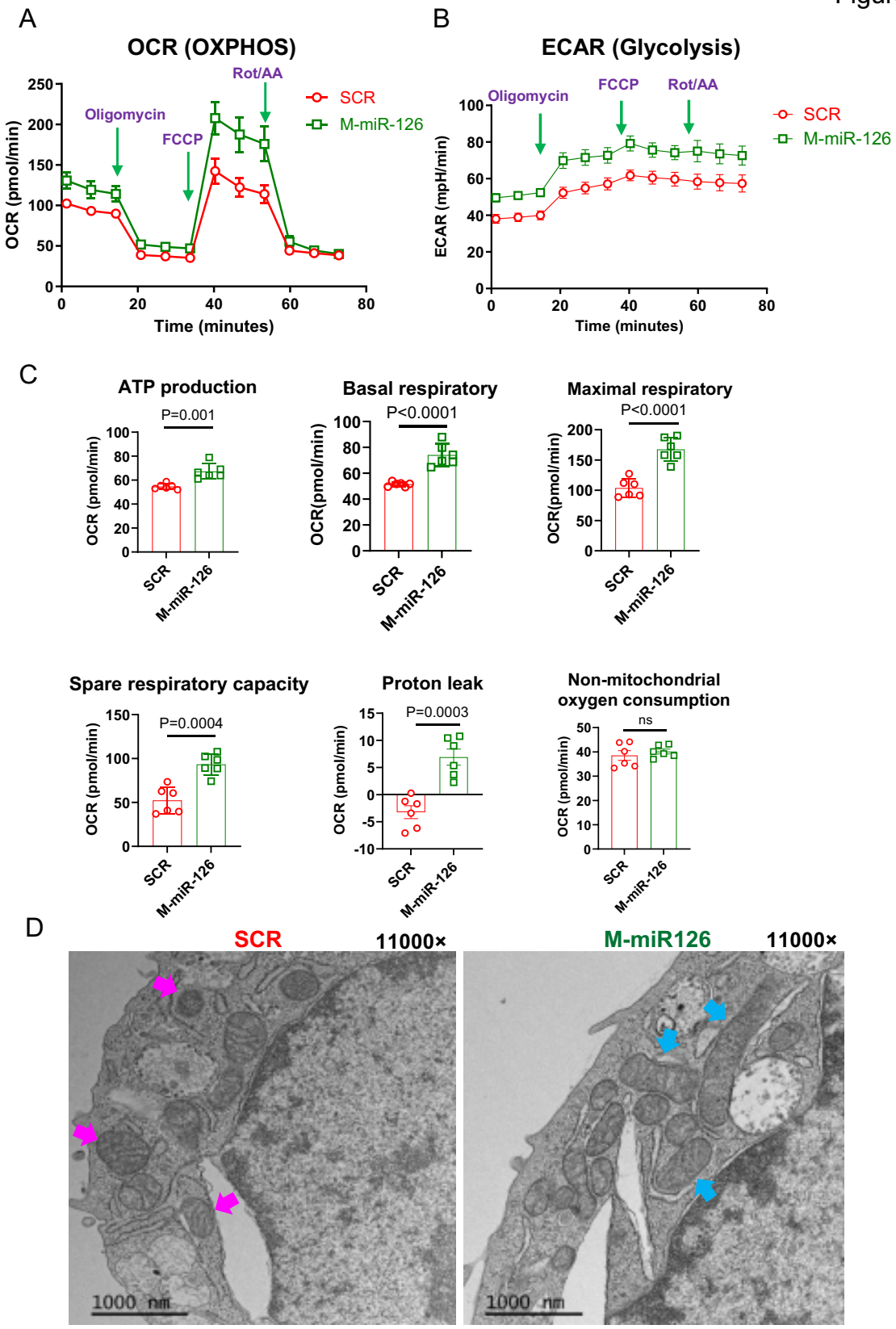
A
OCR (OXPHOS)
OCR (pmol/min)
Time (minutes)
Oligomycin
FCCP
Rot/AA
SCR
M-miR-126
B
ECAR (Glycolysis)
ECAR (mpH/min)
Time (minutes)
Oligomycin
FCCP
Rot/AA
SCR
M-miR-126
C
ATP production
P=0.001
Basal respiratory
P<0.0001
Maximal respiratory
P<0.0001
Spare respiratory capacity
P=0.0004
Proton leak
P=0.0003
Non-mitochondrial oxygen consumption
ns
OCR (pmol/min)
SCR
M-miR-126
D
SCR
11000×
M-miR126
11000×
1000 nm
1000 nm

Figure S17. Seahorse assay and mitochondria imaging of aged HSCs treated with miR-126 mimic

A-C Levels of OCR indicating OXPHOS (**A**) and ECAR indicating glycolysis (**B**) and ATP production, basal respiratory, maximal respiratory, spare respiratory capacity, proton leak, and non-mitochondrial oxygen consumption (**C**) in aged HSCs treated with miR-126 mimic (2μM) or scramble RNA (SCR) for 48 hours, analyzed by seahorse assays. **D** Mitochondria morphology (purple arrows indicate mitochondrial fission; blue arrows indicate mitochondrial fusion) in aged HSCs treated with miR-126 mimic (2μM) or scramble RNA (SCR) for 48 hours, analyzed by electron microscope. Abbreviation: HSC: Lineage-Sca-1+c-Kit+CD150+CD48- hematopoietic stem cells; OCR: oxygen consumption rate; OXPHOS: oxidative phosphorylation; ECAR: extracellular acidification rate; FCCP: carbonyl cyanide-4 (trifluoromethoxy) phenylhydrazone; Rot/AA: rotenone and antimycin A. Comparison between groups was performed by two-tailed, unpaired t-test. Results shown represent mean ± SD. Significance values: ns, not significant.